J. Fluid Mech. (1996), *vol.* 323, *pp.* 133–171

On the weakly nonlinear development of Tollmien–Schlichting wavetrains in boundary layers

By XUESONG WU[1], PHILIP A. STEWART[2] AND STEPHEN J. COWLEY[2]

[1]Department of Mathematics, Imperial College, 180 Queen's Gate, London SW7 2BZ, UK

[2]Department of Applied Mathematics and Theoretical Physics, University of Cambridge, Silver Street, Cambridge CB3 9EW, UK

(Received 27 July 1993 and in revised form 4 April 1996)

The nonlinear development of a weakly modulated Tollmien-Schlichting wavetrain in a boundary layer is studied theoretically using high-Reynolds-number asymptotic methods. The 'carrier' wave is taken to be two-dimensional, and the envelope is assumed to be a slowly varying function of time and of the streamwise and spanwise variables. Attention is focused on the scalings appropriate to the so-called 'upper branch' and 'high-frequency lower branch'. The dominant nonlinear effects are found to arise in the critical layer and the surrounding 'diffusion layer': nonlinear interactions in these regions can influence the development of the wavetrain by producing a spanwise-dependent mean-flow distortion. The amplitude evolution is governed by an integro-partial-differential equation, whose nonlinear term is history-dependent and involves the highest derivative with respect to the spanwise variable. Numerical solutions show that a localized singularity can develop at a finite distance downstream. This singularity seems consistent with the experimentally observed focusing of vorticity at certain spanwise locations, although quantitative comparisons have not been attempted.

1. Introduction

Experimental studies of boundary-layer transition suggest that, in the case of initially small disturbances, there are at least three stages in transition to turbulence. In the first stage, the disturbance may be predominantly two-dimensional, and it evolves according to linear instability theory. In the second stage, three-dimensional components grow rapidly at rates much larger than those predicted by linear theory for the undisturbed basic state. Finally, in the third stage, the flow breaks down into random, small-scale motions. Depending on the initial amplitude, the second stage of development may take different forms. For a relatively large input, Klebanoff & Tidstrom (1959) and Klebanoff, Tidstrom & Sargent (1962) documented that a two-dimensional Tollmien–Schlichting (T-S) wave was warped into a 'peak-valley' pattern, which maintained a fixed spanwise position as it amplified downstream. High-shear layers, followed by 'spikes', were observed to form at the peaks. Transition followed and was characterized by the abrupt growth of disturbances of high frequency and short wavelength. This process is known as 'K-type' transition.

For weaker (quasi-two-dimensional) initial disturbances, however, the rapidly growing three-dimensional waves are found to have a *subharmonic* frequency and a streamwise wavelength approximately twice that of the planar T-S wave; thus, when visualized, the flow field exhibits a staggered pattern (Kachanov & Levchenko 1984; Saric & Thomas 1984). It has been argued that, according to the spanwise wavelength, this process can be subdivided into 'C-type' and 'H-type' transition – where the different classifications refer to the subharmonic-resonance mechanism of Craik (1971) (see also Raetz 1959), and the secondary-instability mechanism of Herbert (1983, 1988), respectively.

K-type transition has, on the whole, received less attention theoretically than the other mechanisms. Herbert (1988) suggested that a fundamental parametric resonance could explain this type of transition. However, except in the case where an exact two-dimensional equilibrium exists, the secondary-instability theory still awaits a fully rigorous mathematical justification (but see Stewart & Smith 1987). Moreover, this approach assumes that the disturbance is spanwise-periodic (as do many other theoretical studies). In flows of practical interest, disturbances can be of a more general form; indeed Gaster & Grant (1975) point out that a wavepacket is a better model of natural transition.

Gaster & Grant (1975) showed experimentally that a wavepacket of small-amplitude disturbances initially evolves according to linear theory. In the linear régime, the wavepacket can be represented as a summation of the least-stable modes (Gaster 1975). At later stages, however, the packet undergoes distortions in which there is a rapid growth of oblique modes with a particular spanwise wavenumber. Gaster & Grant (1975) conjectured that this is the result of nonlinear effects. More recently, Cohen, Breuer & Haritonidis (1991) studied the development of a wavepacket further downstream, and confirmed the observations of Gaster & Grant (1975). Moreover, they concluded that the dominant planar and oblique modes form a resonant triad – a conclusion which is also suggested by figure 9 of Gaster & Grant (1975).

The first theory incorporating nonlinear modulational effects was that of Stewartson & Stuart (1971) for a two-dimensional wavepacket in plane Poiseuille flow (PPF). This work was extended to include spanwise modulation by Hocking *et al.* (1972) and Davey, Hocking & Stewartson (1974) for PPF, and by Hocking (1975) for the asymptotic suction boundary layer. Strictly speaking, however, this approach applies only to exactly parallel flows, since the Reynolds number is taken to be finite. Indeed, most analyses of this type have been performed for Reynolds numbers close to the (finite) critical value for which the flow is marginally stable.

A mathematically self-consistent extension of such weakly nonlinear analyses to spatially varying boundary layers can only be obtained for asymptotically large Reynolds numbers (e.g. Smith 1979; Bodonyi & Smith 1981). There is then a plethora of possible scalings depending on, *inter alia*, the form and size of the initial disturbance. To illustrate this point, consider an infinitesimally small disturbance of fixed frequency, which is propagating downstream. If the disturbance is introduced upstream of the lower branch (e.g. point A in figure 1), it initially decays as it propagates downstream. Once it has passed the lower branch, it starts to grow, and continues to do so until it reaches the upper branch, after which it decays again. By varying the initial amplitude of the disturbance, and the location at which it is introduced, an initially linear perturbation can be made to become nonlinear at virtually any downstream station between the lower and upper branches. The precise evolution of the disturbances depends on where nonlinear effects become important. For instance, a relatively large disturbance may become nonlinear in the lower-

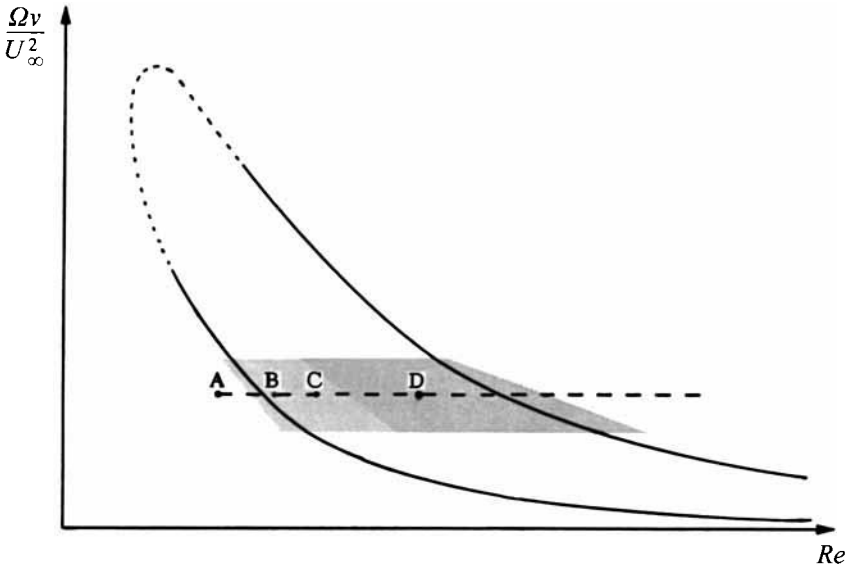

FIGURE 1. Schematic illustration of the different régimes for an experiment where fixed-frequency disturbances are introduced into a flat-plate (or accelerating) boundary layer. The abscissa and ordinate represent downstream distance, and the frequency of the disturbance, respectively. The solid lines represent the asymptotic lower and upper branches of the linear neutral curve, while the dotted line represents the continuation of the neutral curve to finite Reynolds numbers provided by solutions to the (heuristic) Orr–Sommerfeld equation. A fixed-frequency disturbance introduced at point A moves along the dashed line as it propagates downstream. Point C is located in the 'lower-branch' régime (the lightly stippled region), while point B is asymptotically close to the lower neutral curve within this régime. Point D is in the 'upper-branch' régime (the darkly stippled region).

branch region, while a smaller disturbance may remain linear until the upper-branch region.† Furthermore, different forms of nonlinearity result from different types of input disturbance (e.g. predominantly two-dimensional, strongly three-dimensional). Further discussion of this point is given in a recent review by Cowley & Wu (1994).

In this paper we follow Stewartson & Stuart (1971), Hocking *et al.* (1972), etc., and restrict attention to the nonlinear evolution of a slowly modulated wavetrain consisting of (almost) two-dimensional waves. In those early studies, such wavetrains were assumed to develop from initial 'point' perturbations. Here, however, we assume that the weak three-dimensional 'warping' arises from imperfections in the method by which supposedly two-dimensional disturbances are introduced (as is almost inevitable in an experiment). Such three-dimensional effects, though weak, can exert a significant influence on the development of the perturbation.

Modulated disturbances of this kind in boundary layers have been the subject of a number of recent studies. For example, Smith & Walton (1989) have examined

† Definitions of the 'lower-branch' and the 'upper-branch' regions can only be given in an asymptotic sense. For a detailed discussion of this point see, for example, Cowley & Wu (1994). In brief, consider a disturbance with a fixed dimensional frequency, Ω, introduced into an incompressible fluid of kinematic viscosity ν, flowing with velocity U_∞ past an flat plate. Suppose that the frequency parameter, $F = \Omega\nu U_\infty^{-2}$, is small, and that the local (chord-length) Reynolds number, defined by $Re = U_\infty L\nu^{-1}$ where L is the distance from the leading edge, is large. In asymptotic terms, the 'lower-branch region' covers distances from the leading edge where $Re = O(F^{-4/3})$, while the 'upper-branch region' covers the more extensive distances downstream where $Re = O(F^{-5/3})$. These regions are illustrated schematically in figure 1. At finite Reynolds numbers it may be difficult to distinguish between the regions.

the effects of weak spanwise modulation on perturbations which become nonlinear asymptotically close to the lower branch (e.g. point B in figure 1). In particular, their analysis identified the potential for nonlinear interactions between near-planar T-S waves and pre-existing and/or induced longitudinal vortices (see the work of Hall & Smith 1989, 1991 and Smith & Blennerhassett 1992, and references therein, for disturbances with stronger spanwise variations). *Inter alia*, Smith & Walton (1989) showed that the nonlinear amplification of weak three-dimensional warping could lead to the spanwise concentration of streamwise vorticity (see also Hall & Smith 1990 for analogous work on PPF).

There has been little analysis on weakly modulated perturbations that become nonlinear in the major part of the *lower-branch* region, e.g. at points such as C in figure 1. This is because the spatial/temporal growth rate of T-S waves is comparable with the wavenumber/frequency of such waves in this region, with the result that an asymptotic description of nonlinear effects is difficult, if not impossible (e.g. see Hall 1995). However, analytical progress is much more feasible in the *upper-branch* scaling régime (e.g. at points such as D in figure 1), because at high Reynolds numbers, the growth rate of T-S waves in the region is relatively small (e.g. Reid 1965). Further, as Goldstein & Durbin (1986) have observed, this scaling applies to almost the entire linearly unstable region. Therefore, it can be argued that the upper-branch régime is worthy of further study – especially since in many well-known experiments, nonlinear effects are observed to become significant near the upper branch rather than in the vicinity of the lower branch (e.g. Klebanoff *et al.* 1962; Gaster & Grant 1975; Cohen *et al.* 1991).

The 'upstream' limit of the upper-branch scaling matches to the 'downstream' limit of the lower-branch scaling (see below). In the literature the latter limit is sometimes referred to as the 'high-frequency' lower branch (HFLB): see for example Zhuk & Ryzhov (1982), Smith & Burggraf (1985), Smith (1986), Smith & Stewart (1987). Recently, Stewart & Smith (1992) have studied weakly three-dimensional T-S wavetrains in this limit. They make comparisons with the experiments of Klebanoff & Tidstrom (1959), and claim that their wave–vortex-interaction theory 'captures the heart of the experimental findings for this type of boundary-layer transition'. Smith & Bowles (1992) perform the corresponding analysis for PPF, and likewise obtain 'reasonably encouraging' comparisons with the experiments of Nishioka, Asai & Iida (1979). However, in the appropriate 'upstream' limit of our upper-branch analysis, we do not recover the results of Stewart & Smith (1992). The latter are based on the assumption that the critical layer is 'passive', that is, the velocity jump across it is zero (to the required order of working). In Appendix A we show that, for smaller disturbance amplitudes than those considered by Stewart & Smith (1992), there is a nonlinear interaction associated with a non-zero velocity jump across the critical level.† This does not necessarily invalidate the work of Stewart & Smith (1992): if the assumption mentioned above can be justified for larger-amplitude waves, then their analysis may be relevant to certain forms of bypass transition. On the other hand, for small-amplitude disturbances which first becomes nonlinear in the HFLB régime, it would appear that the initial nonlinear stage of development is not described by the Stewart & Smith (1992) theory.

In this paper we develop a self-consistent theory based on a high-Reynolds-number

† We refer to the critical *level*, rather than the critical *layer*, since the thin critical layer is surrounded by a slightly thicker diffusion layer. The key velocity jump is that across the combination of critical layer and diffusion layer.

assumption. We take an flat-plate boundary layer as the basic flow, and concentrate for the most part on the upper-branch régime. The asymptotic description of linear instability then involves a standard five-zone structure (e.g. Bodonyi & Smith 1981). From the standpoint of our weakly nonlinear theory, the zone of most interest is the viscous critical layer, where the velocity of the basic flow is approximately equal to the phase speed of the carrier wave. This layer is surrounded by a quasi-inviscid region (the 'Tollmien layer'), and is thereby separated from the viscous Stokes layer adjacent to the wall. The lower-branch régime, by contrast, has a three-zone ('triple-deck') structure, with a single viscous region (the 'lower deck'): see Appendix A. However, in the 'high-frequency' (or 'downstream') limit of the lower-branch régime, the viscous layer splits into three distinct asymptotic regions: a Stokes layer, a quasi-inviscid layer, and a critical layer (see figure 7). Thus, in this limit, a five-zone structure emerges which matches to that of the upper-branch régime. Indeed, the only significant difference between the HFLB régime and the upper-branch régime is that, in the latter, an extra linear term arises from the curvature of the velocity profile. This means that our analysis for the upper-branch scaling also applies, after trivial modification, to the HFLB scaling (see Appendix A).†

Since the early work of Brown & Stewartson (1978) and Hickernell (1984), nonlinear effects associated with the unsteady evolution of critical layers have been studied extensively, e.g. Churilov & Shukhman (1988), Goldstein & Leib (1989), Goldstein & Choi (1989), Shukhman (1991), Leib (1991), Goldstein & Lee (1992), Wu (1992, 1993*a*), Wu, Lee & Cowley (1993). In all these studies, 'unsteady' inertia terms play a key rôle in the dynamics of the critical layers. Of particular relevance is the work of Wu (1993*a*) on the nonlinear evolution of spanwise-modulated Rayleigh instability waves in the non-equilibrium critical-layer régime. He observes that in the strongly viscous limit, the critical layer splits into two asymptotic regions: an inner quasi-steady viscous critical layer, surrounded by a thicker 'diffusion layer' (see also Brown & Stewartson 1978; Churilov & Shukhman 1987; Wu *et al.* 1993). The existence of the diffusion layer means that, even in this limit, the amplitude equation has a non-local nonlinear term (see also Smith & Walton 1989 and references therein). Wu (1993*a*) points out that this viscous limit is related to the analogous problem for upper-branch T-S waves in boundary layers. The aim of the present paper is to explore this aspect in detail, with extensions to include both a slow streamwise modulation and a slow temporal modulation. In particular, we derive an amplitude equation governing the evolution, with time and/or streamwise distance, of the envelope of a spanwise-modulated wavetrain. Numerical solutions of this equation show that a localized singularity can develop in the solution at a finite distance downstream, with energy and vorticity concentrating at a particular spanwise location. This is possibly in line with the streamwise 'streaks' observed by Klebanoff *et al.* (1962), and others. Although for definiteness the theory is presented for a flat-plate boundary layer, we emphasize that our amplitude equation is in fact generic, and applies to other shear flows as well (e.g. Wu 1993*a*).

This paper is organized as follows. In §2, the problem is formulated. As in Mankbadi, Wu & Lee (1993) and Wu (1993*a*,*b*), we adopt a high-Reynolds-number asymptotic approach. In particular, we identify appropriate 'slow' streamwise and

† A distinguishing feature of the HFLB régime is the fact that, according to linear instability theory, a fixed-frequency disturbance propagating downstream experiences the greatest net increase in amplitude in this intermediate zone between the lower-branch and upper-branch scalings (e.g. Goldstein & Hultgren 1989; Cowley & Wu 1994). This is despite the fact that the local growth rate is larger in the lower-branch régime, and the upper-branch régime extends over a greater distance.

spanwise spatial variables, and also introduce a slow time variable so that a localized wavepacket can (in principle) be described. The mathematical 'book-keeping' then requires the instability to be described by a seven-layer asymptotic structure. Although this multiple-layer formulation may seem unduly elaborate, such an approach ensures that the dominant physical processes are identified and included in the analysis. We find that away from the critical level, nonlinear effects are negligible, and hence a slight extension of the two-dimensional linear analysis of Bodonyi & Smith (1981) gives the leading-order dispersion relation and relates the amplitude growth to the velocity jump across the critical level. In §3, the flow in the critical layer is analysed. It is shown that the flow in this region is viscous and quasi-steady, and that quadratic interactions within the critical layer generate a spanwise-dependent mean-flow correction, which cannot match directly to the outer solution. This indicates the need for a diffusion layer that sandwiches the critical layer (see §4). In the diffusion layer, spatial- and temporal-inertia effects, and viscous effects, all appear at leading order in the governing equations for the induced mean flow. The cubic 'wave–vortex' interaction of this mean flow with the fundamental mode produces a velocity jump across the critical layer and diffusion layer. In §5 the amplitude-evolution equation is obtained, and some of its properties are studied both analytically and numerically. (Appendix B discusses certain limiting cases with weaker or stronger three-dimensionality.) In §6, we relate our results to previous theoretical work, and indicate its possible relevance to experimental observations.

2. Formulation and linear solutions

The basic flow is taken to be the Blasius boundary layer on a flat plate. Cartesian coordinates (x, y, z) are chosen with the origin at a point on the plate a distance L downstream of the leading edge; x is along the plate and y normal to it, while z is in the spanwise direction. The velocity, length, time and pressure are normalized by U_∞, δ^*, δ^*/U_∞ and ρU_∞^2 respectively, where ρ is the fluid density, ν the kinematic viscosity, U_∞ the free-stream velocity, and $\delta^* = (\nu L/U_\infty)^{1/2}$ the boundary-layer thickness at $x = 0$. The local (thickness) Reynolds number $R = U_\infty \delta^*/\nu$ is assumed to be asymptotically large. Close to the wall the basic-flow profile has the expansion

$$U_B \sim \lambda y + \lambda_4 y^4 + \ldots \quad \text{as} \quad y \to 0\,, \tag{2.1}$$

with

$$\lambda = \lambda_0 \left(1 + x/R\right)^{-1/2}, \quad \lambda_4 = -\lambda^2/48\,, \quad \lambda_0 = 0.332\ldots\,. \tag{2.2}$$

Let us suppose that a weakly three-dimensional wavetrain, modulated in the streamwise and spanwise directions, is superimposed upon this base flow. The upper-branch régime corresponds to the scaling

$$R \sim (\Omega \nu/U_\infty^2)^{-5/6}\,, \tag{2.3}$$

where Ω is the dimensional frequency of the carrier wave.† It is convenient to introduce a small parameter $\sigma = R^{-1/10}$, and to define a scaled frequency $\omega =$

† After minor modifications to the asymptotic scalings, our analysis is also applicable to a boundary layer with pressure gradient. In this case, (2.3) should be replaced by $R \sim (\Omega \nu/U_\infty^2)^{-3/4}$. This is the upper-branch scaling for boundary layers with favourable pressure gradients (e.g. Reid 1965; Smith & Bodonyi 1982), but is also relevant to boundary layers with adverse pressure gradients if disturbances become nonlinear when their (linear) growth rate is determined by viscous effects.

$\sigma^{-12}(\Omega\nu/U_\infty^2)$. Linear theory (e.g. Reid 1965; Bodonyi & Smith 1981) suggests the introduction of scaled co-ordinates

$$\xi = \sigma\alpha x - \sigma^2\omega t\,, \quad X = \sigma^4 x\,, \quad T = \sigma^5 t\,, \tag{2.4}$$

where ξ is a 'fast' variable describing the oscillation of planar T-S waves of $O(\sigma^{-1})$ wavelength and $O(\sigma^2)$ frequency, while X and T are 'slow' variables describing the growth of the T-S waves (and the evolution of the wavepacket envelope) over $O(\sigma^{-4})$ distances and $O(\sigma^{-5})$ times. The slow growth is therefore an $O(\sigma^3)$ effect. Following Hocking *et al.* (1972) and others, we fix the scale of the spanwise modulation so that (linear) spanwise dispersion is comparable with the slow growth of the T-S waves. By symmetry, we anticipate that this will be represented by a term of the form $\partial^2/\partial z^2$. Since the wavelength of the T-S waves is $O(\sigma^{-1})$, and the slow growth is an $O(\sigma^3)$ correction, we expect the appropriate spanwise scaling to be

$$Z = \sigma\,\sigma^{3/2} z = \sigma^{5/2} z\,. \tag{2.5}$$

We thus adopt the multiple scales †

$$\frac{\partial}{\partial t} \to -\sigma^2\omega\frac{\partial}{\partial\xi} + \sigma^5\frac{\partial}{\partial T}\,, \quad \frac{\partial}{\partial x} \to \sigma\alpha\frac{\partial}{\partial\xi} + \sigma^4\frac{\partial}{\partial X}\,, \quad \frac{\partial}{\partial z} \to \sigma^{5/2}\frac{\partial}{\partial Z}\,. \tag{2.6}$$

and expand α as

$$\alpha = \alpha_0 + \sigma\alpha_1 + \sigma^2\alpha_2 + \sigma^3 \ln\sigma\alpha_{3L} \tag{2.7}$$

(there is no need for an $O(\sigma^3)$ term since it is accounted for by the slow evolution represented by $\partial/\partial X$). The wave speed is defined as

$$c = \omega/\alpha = c_0 + \sigma c_1 + \sigma^2 c_2 + \dots\,, \quad \text{with} \quad c_0 = \omega/\alpha_0 \quad \text{etc.} \tag{2.8}$$

In terms of these scaled variables, we assume that the wall-pressure perturbation takes the form

$$P = \epsilon\sigma\left\{P_0 + \sigma P_1 + \sigma^2 P_2 + \sigma^3 \ln\sigma P_{3L} + \sigma^3 P_3 + \dots\right\} \mathrm{e}^{\mathrm{i}\xi} + \text{c.c.} + \dots\,, \tag{2.9}$$

where

$$P_i = P_i(X, Z, T)\,, \tag{2.10}$$

and c.c. denotes complex conjugate. It remains to fix the amplitude, ϵ, of the disturbance so that nonlinear effects appear in the leading-order amplitude-evolution equation. We consider this point after briefly outlining the asymptotic structure of the solution (see (2.31) below).

As pointed out by Bodonyi & Smith (1981), the linear instability problem is described by a multi-layer structure with five asymptotic regions: the potential-flow zone (I), the main layer (II), the Tollmien layer (III), the Stokes layer (IV), and the critical layer (V). These layers have thickness of order σ^{-1}, 1, σ, σ^4 and σ^3 respectively. However, when nonlinear effects are included it turns out that, in addition, a diffusion layer (VI) and a wall-buffer layer (VII) have to be introduced (cf. Wu 1993*b*). The structure thus consists of seven zones, as shown in figure 2. We obtain the solution in each of the regions by expanding in terms of the small parameter σ. In layers (I)–(IV), this procedure is straightforward since little more than the linear analysis

† Strictly speaking, there should be an extra $O(\sigma^{10})$ term in the streamwise scaling in order to represent the very 'slow' non-parallelism of the boundary layer. However, this term has been suppressed since it does not enter the calculation to the order required; in other words, we may neglect the x-dependence of the basic flow U_B, and use $\lambda = \lambda_0$ in place of (2.2).

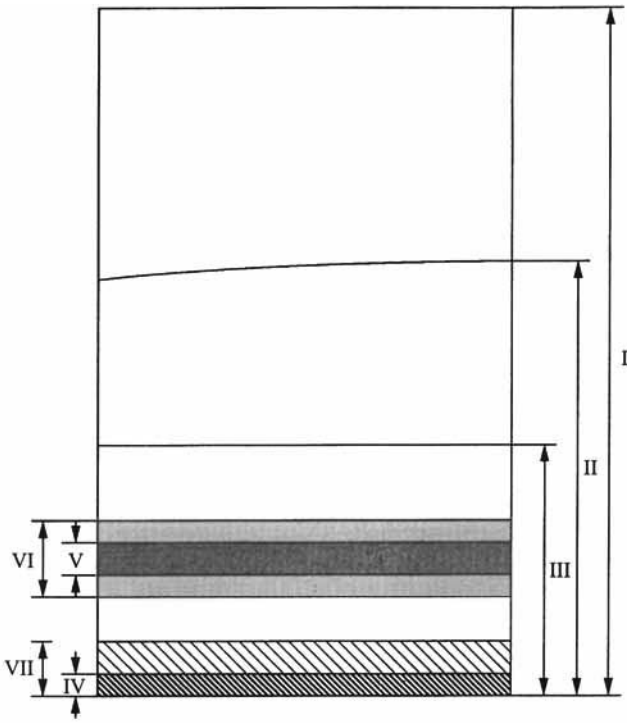

FIGURE 2. Schematic of the seven-zone flow structure: the potential layer I, the main layer II, the Tollmien layer III, the Stokes layer IV, the critical layer V, the diffusion layer VI and the wall-buffer layer VII. These layers have thicknesses $O(\sigma^{-1})$, $O(1)$, $O(\sigma)$, $O(\sigma^4)$, $O(\sigma^3)$, $O(\sigma^{5/2})$ and $O(\sigma^{5/2})$ respectively (in the case of a purely spatial stability analysis, the wall-buffer layer has width $O(\sigma^2)$).

of Bodonyi & Smith (1981) is required. The key regions are those where nonlinear dynamics plays an essential part, namely, the critical layer (V) and the diffusion layer (VI). These will be considered in §3 and §4 respectively. (The wall-buffer layer (VII) has a purely passive rôle, and will not be discussed further.)

We first consider the Tollmien layer (III), where the appropriate normal coordinate is

$$Y = y/\sigma\,, \tag{2.11}$$

and the flow is effectively inviscid. The perturbation velocity components corresponding to (2.9) expand in the form

$$u = \epsilon\left\{U_0 + \sigma U_1 + \sigma^2 U_2 + \sigma^3 \log\sigma U_{3L} + \sigma^3 U_3 + \ldots\right\} e^{i\xi} + \text{c.c.} + \ldots\,, \tag{2.12}$$

$$v = \epsilon\sigma^2\left\{V_{0+} + \sigma V_1 + \sigma^2 V_2 + \sigma^3 \log\sigma V_{3L} + \sigma^3 V_3 + \ldots\right\} e^{i\xi} + \text{c.c.} + \ldots\,, \tag{2.13}$$

$$w = \epsilon\sigma^{3/2}\left\{W_0 + \ldots\right\} e^{i\xi} + \text{c.c.} + \ldots\,, \tag{2.14}$$

where

$$U_i = U_i(T, X, Y, Z)\,, \quad \text{etc.} \tag{2.15}$$

With ϵ specified by (2.31), nonlinear terms do not occur in the governing equations to the order shown. The solutions for $U_i, V_i, i = 0, 1, 2, 3L$ are exactly as in the

two-dimensional analysis of Bodonyi & Smith (1981), namely

$$U_0 = \lambda A_0 \,, \quad V_0 = -\mathrm{i}\alpha_0 \lambda A_0 Y \,, \tag{2.16}$$

$$U_1 = \lambda \left(A_1 - \frac{\alpha_1}{\alpha_0} A_0 \right) \,, \quad V_1 = -\mathrm{i}\alpha_0 \lambda A_1 Y \,, \tag{2.17}$$

$$U_2 = \lambda \left(A_2 - \frac{\alpha_1}{\alpha_0} A_1 - \frac{\alpha_2}{\alpha_0} A_0 + \frac{\alpha_1^2}{\alpha_0^2} A_0 \right) \,, \quad V_2 = -\mathrm{i}\alpha_0 \lambda A_2 Y \,, \tag{2.18}$$

$$U_{3L} = \lambda \left(A_{3L} - \frac{\alpha_{3L}}{\alpha_0} A_0 \right) \,, \quad V_{3L} = -\mathrm{i}\alpha_0 \lambda A_{3L} Y \,, \tag{2.19}$$

with

$$A_0 = \frac{\alpha_0 P_0}{\lambda \omega} \,, \quad A_1 = \frac{\alpha_0 P_1 + 2\alpha_1 P_0}{\lambda \omega} \,, \tag{2.20}$$

$$A_2 = \frac{1}{\lambda \omega} \left\{ \alpha_0 P_2 + 2\alpha_1 P_1 + \left(2\alpha_2 + \frac{\alpha_1^2}{\alpha_0} \right) P_0 \right\} \,, \quad A_{3L} = \frac{\alpha_0 P_{3L} + 2\alpha_{3L} P_0}{\lambda \omega} \,. \tag{2.21}$$

Here, however, there is a spanwise velocity whose leading-order component is given by

$$W_0 = -\frac{1}{\mathrm{i}\alpha_0 (\lambda Y - c_0)} \frac{\partial P_0}{\partial Z} \,, \tag{2.22}$$

and the three-dimensionality makes its presence felt in the equations for U_3 and V_3; it is found that

$$\begin{aligned} V_3 = {} & -\mathrm{i}\alpha_0 \lambda A_3 (Y - \hat{c}) + B_3 \\ & -\mathrm{i}\alpha_0 \lambda_4 A_0 \left(Y^4 + 2\hat{c} Y^3 + 6\hat{c}^2 Y^2 + 12\hat{c}^3 (Y - \hat{c}) \ln (Y - \hat{c}) \right) \,, \end{aligned} \tag{2.23}$$

where we define

$$\hat{c} = c_0 / \lambda \,, \tag{2.24}$$

and

$$B_3 = -\frac{1}{\lambda} \left\{ \mathrm{i}\alpha_0 P_3 + \frac{\partial P_0}{\partial X} + \frac{\partial U_0}{\partial T} + c_0 \frac{\partial U_0}{\partial X} + \frac{1}{\mathrm{i}\alpha_0} \frac{\partial^2 P_0}{\partial Z^2} \right\} \tag{2.25}$$

is a function of T, X and Z only, as is the unknown A_3. We note that V_3 exhibits the familiar logarithmic branch-point singularity at $Y = \hat{c}$, i.e. where the basic-flow velocity equals the wave speed to leading order. This gives rise to the *critical layer* (V), in which viscosity acts to smooth out the solution. The logarithm in (2.23) is to be interpreted as

$$\ln (Y - \hat{c}) = \begin{cases} \ln |Y - \hat{c}| \,, & Y > \hat{c} \,, \\ \ln |Y - \hat{c}| - \mathrm{i}\phi \,, & Y < \hat{c} \,, \end{cases} \tag{2.26}$$

where the so-called *phase shift*

$$\phi \equiv \frac{1}{12 \lambda_4 \alpha_0 \hat{c}^3 A_0} \left[\frac{\partial V_3}{\partial Y} \right]_{Y = \hat{c}^-}^{Y = \hat{c}^+} \tag{2.27}$$

is determined from the critical-layer solution.

The expansions of velocity and pressure in the potential-flow zone (I), main layer (II) and Stokes layer (IV) develop in a similar way to (2.9) and (2.12)–(2.14). Since the governing equations are again linear to the required order of working, solutions may be obtained by a straightforward modification of Bodonyi & Smith's (1981) analysis

and are not presented here. From matching the leading-order solutions in regions (I)–(IV) we obtain the leading-order dispersion relation

$$\alpha_0 = (\lambda\omega)^{1/2} \ . \tag{2.28}$$

Matching at higher order yields the wavenumber corrections α_i, $i = 1, 2, 3L$ (which will not concern us here), and an equation for the evolution of the wall-pressure amplitude, namely

$$\frac{\partial P_0}{\partial T} + c_g \frac{\partial P_0}{\partial X} - \mathrm{i}\, d \frac{\partial^2 P_0}{\partial Z^2} = \check{\kappa} P_0 + 12\lambda_4 \alpha_0 \hat{c}^4 \phi P_0 \ ; \tag{2.29}$$

the group velocity c_g and dispersion parameter d are given by

$$c_g = 2c_0 \quad \text{and} \quad d = (2\lambda)^{-1} \ , \quad \text{and} \quad \mathrm{Re}(\check{\kappa}) = \lambda\alpha_0/(2\omega)^{1/2} = \left(\lambda^3/2\right)^{1/2} \tag{2.30}$$

is the viscous growth rate associated with the Stokes layer. The value of $\mathrm{Im}(\check{\kappa})$ need not concern us since it can be scaled out of the final amplitude equation: see (5.7) and (5.8). The important final term of (2.29) represents the contribution from ϕ, the phase shift across the critical layer; it is here that nonlinearity can enter the governing equation (2.29). In the linear régime $\phi \equiv \pi$, and this final term has a stabilizing effect, since λ_4, the curvature of the basic flow profile, is negative.

As can be seen from (2.22), the three-dimensionality, though weak, forces a simple pole singularity in the leading-order spanwise velocity W_0 at the critical level $Y = \hat{c}$. It is this property that dictates the form of the nonlinear interactions inside the critical layer and the diffusion layer, and fixes the amplitude ϵ for which nonlinear effects are as important as the weak linear growth effects. A scaling argument similar to that given by Wu (1993*a*) shows that nonlinear interactions affect the phase shift ϕ when

$$\epsilon \sim \sigma^{25/4} \ , \tag{2.31}$$

as will become apparent once the critical-layer and diffusion-layer solutions have been presented (§§3–4). We note that the scaling (2.31) is asymptotically smaller than the $O(\sigma^5)$ amplitude at which the critical layer of a purely two-dimensional disturbance becomes strongly nonlinear (cf. Haberman 1972). For two-dimensional perturbations of that size, Goldstein & Durbin (1986) show that the upper branch of the neutral curve can be eliminated. However, as we shall see, weak three-dimensional effects can lead to a nonlinear interaction different from that of Goldstein & Durbin (1986), and cause a radical departure from linear behaviour for disturbances whose amplitude scales as in (2.31).

3. Critical-layer dynamics

Within the critical layer, as for a linear T-S wave, there is a leading-order balance between the viscous and quasi-steady inertia terms (nonlinear effects enter at higher order). The appropriate transverse variable in this layer is therefore

$$\eta = (y - y_c)/\sigma^3 \ , \quad y_c = \sigma c/\lambda \ , \tag{3.1}$$

and the expansions consistent with (2.31) are

$$\begin{aligned} u = {} & \sigma^{25/4}\left\{\bar{U}_0 + \sigma\bar{U}_1 + \sigma^2\bar{U}_2 + \sigma^{5/2}\bar{U}_{5/2} + \sigma^3 \ln\sigma\, \bar{U}_{3L} + \sigma\bar{U}_3 + \ldots\right\} \mathrm{e}^{\mathrm{i}\xi} \\ & + \sigma^{17/2}\left\{\bar{U}_{II}^{(0)} + \ldots\right\} \mathrm{e}^{2\mathrm{i}\xi} + \mathrm{c.c.} \\ & + \sigma^7 \bar{U}_M^{(0)} + \sigma^{15/2}\bar{U}_M^{(1)} + \sigma^8 \bar{U}_M^{(2)} + \sigma^{17/2} \ln\sigma\, \bar{U}_M^{(3L)} + \sigma^{17/2}\bar{U}_M^{(3)} + \ldots \ , \end{aligned} \tag{3.2}$$

$$v = \sigma^{33/4}\{\bar{V}_{-2} + \sigma\bar{V}_{-1} + \sigma^2\bar{V}_0 + \sigma^3\bar{V}_1 + \sigma^4\bar{V}_2 + \sigma^{9/2}\bar{V}_{5/2} + \sigma^5 \ln\sigma\bar{V}_{3L}$$
$$+\sigma^5\bar{V}_3 + \ldots\}\,\mathrm{e}^{\mathrm{i}\xi}$$
$$+\sigma^{25/2}\left\{\bar{V}_{II}^{(0)} + \ldots\right\}\mathrm{e}^{2\mathrm{i}\xi} + \text{c.c.} + \sigma^{12}\bar{V}_M^{(2)} + \sigma^{25/2}\ln\sigma\,\bar{V}_M^{(3L)} + \sigma^{25/2}\bar{V}_M^{(3)} + \ldots\,, \tag{3.3}$$

$$w = \sigma^{23/4}\{\bar{W}_0 + \ldots\}\,\mathrm{e}^{\mathrm{i}\xi} + \sigma^7\left\{\bar{W}_{II}^{(0)} + \ldots\right\}\mathrm{e}^{2\mathrm{i}\xi} + \text{c.c.}$$
$$+\sigma^7\ln\sigma\,\bar{W}_M^{(3L)} + \sigma^7\bar{W}_M^{(3)} + \sigma^{15/2}\bar{W}_M^{(4)} + \ldots\,, \tag{3.4}$$

together with (2.9) as the expansion for the pressure. It is found that

$$\bar{V}_{-2} = -\mathrm{i}\alpha_0 c_0 A_0\,, \quad \bar{V}_{-1} = -\mathrm{i}\alpha_0(c_0A_1 + c_1A_0)\,, \tag{3.5}$$

$$\bar{V}_0 = -\mathrm{i}\alpha_0(c_0A_2 + c_1A_1 + c_2A_0) - \mathrm{i}\,\alpha_0\lambda A_0\eta\,, \tag{3.6}$$

and that $\bar{W}_0$ satisfies

$$\left(\mathrm{i}\alpha_0\lambda\eta - \frac{\partial^2}{\partial\eta^2}\right)\bar{W}_0 = -\frac{\partial P_0}{\partial Z}\,, \tag{3.7}$$

so that

$$\bar{W}_0 = -\frac{1}{\alpha_0\lambda}\frac{\partial P_0}{\partial Z}\int_0^\infty \mathrm{e}^{-\mathrm{i}q\eta - sq^3}\,\mathrm{d}q\,, \quad s = \frac{1}{3\alpha_0\lambda}\,. \tag{3.8}$$

It turns out that the key nonlinear effect is the interaction of the fundamental mode, $\mathrm{e}^{\mathrm{i}\xi}$, with the induced mean-flow correction represented by the $\bar{U}_M^{(i)}$, $\bar{V}_M^{(i)}$, and $\bar{W}_M^{(i)}$. The second-harmonic ($\mathrm{e}^{2\mathrm{i}\xi}$) terms are too small in magnitude to contribute to the leading-order amplitude equation, and will not be discussed here.

The mean-flow-correction terms satisfy

$$\frac{\partial^2\bar{U}_M^{(0)}}{\partial\eta^2} = 0 \quad ; \quad \frac{\partial^2\bar{U}_M^{(1)}}{\partial\eta^2} = 0\,; \tag{3.9}$$

$$\frac{\partial\bar{V}_M^{(2)}}{\partial\eta} = 0 \quad , \quad \frac{\partial^2\bar{U}_M^{(2)}}{\partial\eta^2} = \lambda\bar{V}_M^{(2)} + \left(\frac{\partial}{\partial T} + c_0\frac{\partial}{\partial X}\right)\bar{U}_M^{(0)}\,; \tag{3.10}$$

$$\frac{\partial\bar{V}_M^{(3L)}}{\partial\eta} + \frac{\partial\bar{W}_M^{(3L)}}{\partial Z} = 0 \quad , \quad \frac{\partial^2\bar{U}_M^{(3L)}}{\partial\eta^2} = \lambda\bar{V}_M^{(3L)} \quad , \quad \frac{\partial^2\bar{W}_M^{(3L)}}{\partial\eta^2} = 0\,; \tag{3.11}$$

$$\frac{\partial\bar{V}_M^{(3)}}{\partial\eta} + \frac{\partial\bar{W}_M^{(3)}}{\partial Z} = 0\,, \quad \frac{\partial^2\bar{U}_M^{(3)}}{\partial\eta^2} = \lambda\bar{V}_M^{(3)} + \left(\frac{\partial}{\partial T} + c_0\frac{\partial}{\partial X}\right)\bar{U}_M^{(1)}\,, \tag{3.12}$$

$$\frac{\partial^2\bar{W}_M^{(3)}}{\partial\eta^2} = \bar{V}_{-2}^*\frac{\partial\bar{W}_0}{\partial\eta} + \text{c.c.}\,; \quad \frac{\partial^2\bar{W}_M^{(4)}}{\partial\eta^2} = 0 \quad ; \quad \text{etc.} \tag{3.13}$$

The only nonlinear forcing term in these equations is the right-hand side of the first of (3.13), which represents the leading-order Reynolds stress of the T-S wave. After substitution from (3.5) and (3.8), this equation can be solved to give

$$\bar{W}_M^{(3)} = \frac{1}{\lambda^2}P_0^*\frac{\partial P_0}{\partial Z}\int_0^\infty\{\mathrm{e}^{-\mathrm{i}q\eta} - 1\}\frac{\mathrm{e}^{-sq^3}}{q}\,\mathrm{d}q + \text{c.c.}$$
$$+\bar{w}_{M0}^{(3)}(T,X,Z) + \eta\bar{\mu}_M^{(3)}(T,X,Z) \tag{3.14}$$

It follows that as $\eta \to \pm\infty$,

$$\bar{W}_M^{(3)} \sim \eta\bar{\mu}_M^{(3)} - \frac{\ln|\eta|}{\lambda^2}\frac{\partial}{\partial Z}(|P_0|^2) + D_\pm(T,X,Z) + o(1)\,, \tag{3.15}$$

with

$$D_+ - D_- = -\frac{\mathrm{i}\pi}{\lambda^2} P_0^* \frac{\partial P_0}{\partial Z} + \text{c.c.} \tag{3.16}$$

In the Tollmien layer, however, the Z-component of mean flow can be no larger than $O(\sigma^{10})$; direct matching with the critical-layer solution is therefore impossible. However, this is a familiar problem in critical-layer theory, first identified (for a two-dimensional flow) by Brown & Stewartson (1978) (see also Churilov & Shukhman 1987; Goldstein & Hultgren 1988). The difficulty arises because the critical-layer equations are *quasi-steady* to leading order, and generate what appears to be a steady mean flow. However, in a problem where the disturbance evolves from an infinitesimal state, it is clear that the mean flow must also evolve on the same slow timescale. The viscous critical layer can therefore be regarded as a region of forcing, away from which the mean flow diffuses on the slow evolution timescale (see also Wu 1993*a*, Wu *et al.* 1993). From balancing the $\sigma^5 \partial/\partial T$ unsteady term with the $\sigma^{10}\partial^2/\partial y^2$ viscous term, the 'diffusion layer' which sandwiches the critical layer is seen to have an $O(\sigma^{5/2})$ thickness.

The diffusion-layer solution will be presented in the next section. It turns out that the Z-component of mean flow in the diffusion layer cannot be larger than $O(\sigma^7)$. Thus it is required that

$$\bar{\mu}_M^{(3)} = 0\,, \quad \bar{W}_M^{(3L)} = \frac{1}{\lambda^2}\frac{\partial}{\partial Z}(|P_0|^2)\,. \tag{3.17}$$

Further, the $O(\sigma^7)$ crossflow induces a streamwise mean-flow correction of the same order in the diffusion layer. This necessitates the introduction of the additional mean-flow terms $\bar{U}_0, \bar{U}_1, \bar{U}_2, \bar{V}_2$ in the critical layer; these are of the form

$$\bar{U}_M^{(0)} = \bar{u}_{M0}^{(0)}(T,X,Z)\,; \tag{3.18}$$

$$\bar{U}_M^{(1)} = \bar{u}_{M0}^{(1)}(T,X,Z) + \eta\bar{\lambda}_M^{(1)}(T,X,Z)\,; \tag{3.19}$$

$$\bar{V}_M^{(2)} = \bar{v}_{M0}^{(2)}(T,X,Z)\,, \tag{3.20}$$

$$\bar{U}_M^{(2)} = \bar{u}_{M0}^{(2)}(T,X,Z) + \eta\bar{\lambda}_M^{(2)}(T,X,Z) + \frac{1}{2}\eta^2\left\{\left(\frac{\partial}{\partial T} + c_0\frac{\partial}{\partial X}\right)\bar{u}_{M0}^{(0)} + \lambda\bar{v}_{M0}^{(2)}\right\}. \tag{3.21}$$

The functions $\bar{u}_{M0}^{(i)}$, $\bar{v}_{M0}^{(i)}$, $\bar{\lambda}_M^{(i)}$ are arbitrary at this stage, and are subsequently determined by matching.

It remains to solve for the higher-order fundamental components $\bar{U}_i$, $\bar{V}_i$ for $i = 1,2,\ldots$, and to calculate the velocity jumps $J_C^{(i)}$, defined by

$$J_C^{(i)} = \int_{-\infty}^{\infty} \frac{\partial^2 \bar{V}_i}{\partial \eta^2}\,\mathrm{d}\eta\,, \tag{3.22}$$

where the integral is to be interpreted as a Hadamard finite part. It is found that

$$J_C^{(1)} = J_C^{(2)} = J_C^{(5/2)} = J_C^{(3L)} = 0\,. \tag{3.23}$$

At next order, however, the relevant equations are

$$\mathrm{i}\alpha_0\bar{U}_3 + \frac{\partial \bar{V}_3}{\partial \eta} = \text{o.l.t}\,, \tag{3.24}$$

$$\left(\mathrm{i}\alpha_0\lambda\eta - \frac{\partial^2}{\partial\eta^2}\right)\bar{U}_3 + \bar{V}_3 = -\bar{V}_{-2}\left\{2\lambda_4\hat{c}^2\eta + \frac{\partial \bar{U}_M^{(2)}}{\partial\eta}\right\} + \text{o.l.t}\,, \tag{3.25}$$

where o.l.t. stands for other linear terms which do not contribute to the jump in $\partial\bar{V}_3/\partial\eta$. After use of (3.5) and (3.21), this key velocity jump is found to be given by

$$J_C^{(3)} = 12\pi\lambda_4\alpha_0\hat{c}^3A_0 + \pi\alpha_0\hat{c}A_0\left\{\left(\frac{\partial}{\partial T} + c_0\frac{\partial}{\partial X}\right)\bar{u}_{M0}^{(0)} + \lambda\bar{v}_{M0}^{(2)}\right\} . \tag{3.26}$$

The first term in (3.26) is linear, while the second represents the leading-order nonlinear interaction of the fundamental mode with the induced mean-flow correction.

4. Diffusion-layer dynamics

As pointed out in the previous section, it is necessary to introduce a diffusion layer, of thickness $O(\sigma^{5/2})$, to accommodate the mean-flow distortion. We thus define

$$\tilde{\eta} = (y - y_c)/\sigma^{5/2} = \sigma^{1/2}\eta , \tag{4.1}$$

and make the expansions

$$\begin{aligned} u = {} & \sigma^{25/4}\{\tilde{U}_0 + \sigma\tilde{U}_1 + \sigma^{3/2}\tilde{U}_{3/2} + \sigma^2\tilde{U}_2 + \sigma^3\ln\sigma\tilde{U}_{3L} + \sigma^3\tilde{U}_3 + \ldots\}\,\mathrm{e}^{\mathrm{i}\xi} \\ & + \sigma^{10}\left\{\tilde{U}_{II}^{(0)} + \ldots\right\}\mathrm{e}^{2\mathrm{i}\xi} + \text{c.c.} + \sigma^7\tilde{U}_M + \ldots , \end{aligned} \tag{4.2}$$

$$\begin{aligned} v = {} & \sigma^{33/4}\{\tilde{V}_{-3/2} + \sigma\tilde{V}_{-1/2} + \sigma^{3/2}\tilde{V}_0 + \sigma^{5/2}\tilde{V}_1 \\ & + \sigma^3\tilde{V}_{3/2} + \sigma^{7/2}\tilde{V}_2 + \sigma^{9/2}\ln\sigma\tilde{V}_{3L} + \sigma^{9/2}\tilde{V}_3 + \ldots\}\,\mathrm{e}^{\mathrm{i}\xi} \\ & + \sigma^{27/2}\left\{\tilde{V}_{II}^{(0)} + \ldots\right\}\mathrm{e}^{2\mathrm{i}\xi} + \text{c.c.} + \sigma^{12}\tilde{V}_M + \ldots , \end{aligned} \tag{4.3}$$

$$w = \sigma^{25/4}\{\tilde{W}_0 + \ldots\}\,\mathrm{e}^{\mathrm{i}\xi} + \sigma^{17/2}\left\{\tilde{W}_{II}^{(0)} + \ldots\right\}\mathrm{e}^{2\mathrm{i}\xi} + \text{c.c.} + \sigma^7\tilde{W}_M + \ldots , \tag{4.4}$$

where the subscript M is again used to indicate contributions to the mean flow.† It is found that

$$\tilde{V}_{-3/2} = -\mathrm{i}\alpha_0 c_0 A_0 , \quad \tilde{V}_{-1/2} = -\mathrm{i}\alpha_0(c_0A_1 + c_1A_0) , \tag{4.5}$$

$$\tilde{U}_0 = \lambda A_0 , \quad \tilde{V}_0 = -\mathrm{i}\alpha_0\lambda A_0\tilde{\eta} , \quad \tilde{W}_0 = -\frac{1}{\mathrm{i}\alpha_0\lambda\tilde{\eta}}\frac{\partial P_0}{\partial Z} , \tag{4.6}$$

and that the governing equations for $\tilde{U}_M$, $\tilde{V}_M$ and $\tilde{W}_M$ are (cf. Hall & Smith 1990)

$$\frac{\partial\tilde{V}_M}{\partial\tilde{\eta}} + \frac{\partial\tilde{W}_M}{\partial Z} = 0 , \tag{4.7}$$

$$\left(\frac{\partial}{\partial T} + c_0\frac{\partial}{\partial X} - \frac{\partial^2}{\partial\tilde{\eta}^2}\right)\tilde{U}_M + \lambda\tilde{V}_M = -\tilde{V}_{-3/2}^{*}\frac{\partial\tilde{U}_0}{\partial\tilde{\eta}} + \text{c.c.} = 0 , \tag{4.8}$$

$$\begin{aligned} \left(\frac{\partial}{\partial T} + c_0\frac{\partial}{\partial X} - \frac{\partial^2}{\partial\tilde{\eta}^2}\right)\tilde{W}_M &= -\tilde{V}_{-3/2}^{*}\frac{\partial\tilde{W}_0}{\partial\tilde{\eta}} + \text{c.c.} \\ &= -\frac{1}{\lambda^2\tilde{\eta}^2}P_0^{*}\frac{\partial P_0}{\partial Z} + \text{c.c.} \end{aligned} \tag{4.9}$$

† As mentioned in the previous section, there is no mean-flow term of order $\sigma^7\ln\sigma$ in expansion (4.4), contrary to what is implied by Wu (1993*a*), §6.2. (The expansions immediately before equation (6.6) of that paper should not contain the logarithmic terms $\tilde{U}_1$, $\tilde{V}_1$ and $\tilde{W}_1$. This has no bearing on the rest of the paper, however.)

We note that both spatial and temporal variation appears at leading order in the mean-flow equations. Equation (4.9) is to be solved subject to the requirement that

$$\tilde{W}_M \to 0 \quad \text{as} \quad |\tilde{\eta}| \to \infty\,, \tag{4.10}$$

and the jump conditions across $\tilde{\eta} = 0$

$$\left[\tilde{W}_M + \frac{\ln|\tilde{\eta}|}{\lambda^2}\frac{\partial}{\partial Z}(|P_0|^2)\right]_{\tilde{\eta}=0^-}^{\tilde{\eta}=0^+} = -\frac{\mathrm{i}\pi}{\lambda^2}P_0^*\frac{\partial P_0}{\partial Z} + \text{c.c.} \tag{4.11}$$

$$\left[\frac{\partial \tilde{W}_M}{\partial \tilde{\eta}} + \frac{1}{\lambda^2\tilde{\eta}}\frac{\partial}{\partial Z}(|P_0|^2)\right]_{\tilde{\eta}=0^-}^{\tilde{\eta}=0^+} = 0\,, \tag{4.12}$$

in view of (3.15) and the second of (3.13). The solution can be expressed in the form

$$\tilde{W}_M = \frac{1}{\lambda^2 c_0}\int_0^\infty\int_0^\infty F(T-\zeta/c_0, X-\zeta, Z)\, k\mathrm{e}^{-k^2\zeta/c_0 - \mathrm{i}k\tilde{\eta}}\,\mathrm{d}k\,\mathrm{d}\zeta + \text{c.c.}\,, \tag{4.13}$$

where

$$F(T,X,Z) = P_0^*\frac{\partial P_0}{\partial Z}\,. \tag{4.14}$$

Equations (4.7) and (4.8) can then be solved, subject to matching with (3.18)–(3.20), to give

$$\begin{aligned}\tilde{V}_M = &-\frac{\mathrm{i}}{\lambda^2 c_0}\int_0^\infty\int_0^\infty F_Z(T-\zeta/c_0, X-\zeta, Z)\,\mathrm{e}^{-k^2\zeta/c_0 - \mathrm{i}k\tilde{\eta}}\,\mathrm{d}k\,\mathrm{d}\zeta \\ &+ \text{c.c.} - \frac{1}{\lambda}\left(\frac{\partial}{\partial T} + c_0\frac{\partial}{\partial X}\right)\tilde{u}_M(T,X,Z)\,,\end{aligned} \tag{4.15}$$

$$\begin{aligned}\tilde{U}_M = &\frac{\mathrm{i}}{\lambda c_0^2}\int_0^\infty\int_0^\infty \zeta\, F_Z(T-\zeta/c_0, X-\zeta, Z)\,\mathrm{e}^{-k^2\zeta/c_0 - \mathrm{i}k\tilde{\eta}}\,\mathrm{d}k\,\mathrm{d}\zeta \\ &+ \text{c.c.} + \tilde{u}_M(T,X,Z)\,.\end{aligned} \tag{4.16}$$

The function $\tilde{u}_M$ is arbitrary at this stage, but does not affect the amplitude-evolution equation. By matching the mean-flow solutions (4.15)–(4.16) to those in the critical layer, it is possible to determine some of the arbitrary functions appearing in (3.18)–(3.21). For our purposes, we need merely note that

$$\begin{aligned}\bar{u}_{M0}^{(0)} = &\frac{\mathrm{i}}{\lambda c_0^2}\int_0^\infty\int_0^\infty \zeta\, F_Z(T-\zeta/c_0, X-\zeta, Z)\,\mathrm{e}^{-k^2\zeta/c_0}\,\mathrm{d}k\,\mathrm{d}\zeta \\ &+ \text{c.c.} + \tilde{u}_M(T,X,Z)\,,\end{aligned} \tag{4.17}$$

$$\begin{aligned}\bar{v}_{M0}^{(2)} = &-\frac{\mathrm{i}}{\lambda^2 c_0}\int_0^\infty\int_0^\infty F_Z(T-\zeta/c_0, X-\zeta, Z)\,\mathrm{e}^{-k^2\zeta/c_0}\,\mathrm{d}k\,\mathrm{d}\zeta \\ &+ \text{c.c.} - \frac{1}{\lambda}\left(\frac{\partial}{\partial T} + c_0\frac{\partial}{\partial X}\right)\tilde{u}_M(T,X,Z)\,,\end{aligned} \tag{4.18}$$

which can be substituted into (3.26) to determine the velocity jump $J_C^{(3)}$.

Finally, we solve for the higher-order fundamental amplitudes $\tilde{U}_i$, $\tilde{V}_i$, $\tilde{W}_i$, $i = 1, \frac{3}{2}, \ldots$, and determine the velocity jumps across the diffusion layer, namely

$$J_D^{(i)} = \int_{-\infty}^{\infty}\frac{\partial^2\tilde{V}_i}{\partial\tilde{\eta}^2}\,\mathrm{d}\tilde{\eta}\,, \tag{4.19}$$

where once again the Hadamard finite part is understood. It is found that

$$J_D^{(1)} = J_D^{(3/2)} = J_D^{(2)} = J_D^{(3L)} = 0 \,. \tag{4.20}$$

However, the mean-flow correction (4.16) interacts with the fundamental mode to force the $O(\sigma^{25/4}\sigma^3)$ streamwise velocity $\tilde{U}_3$, which satisfies

$$\mathrm{i}\alpha_0\tilde{U}_3 + \frac{\partial\tilde{V}_3}{\partial\tilde{\eta}} = \text{o.l.t.}\,, \quad \mathrm{i}\alpha_0\lambda\tilde{\eta}\tilde{U}_3 + \lambda\tilde{V}_3 = -\tilde{V}_{-3/2}\frac{\partial\tilde{U}_M}{\partial\tilde{\eta}} + \text{o.l.t.} \tag{4.21}$$

In consequence there is a velocity jump in $\partial\tilde{V}_3/\partial\tilde{\eta}$, given by

$$J_D^{(3)} = \frac{\mathrm{i}\pi^{3/2}\alpha_0\hat{c}A_0}{4\lambda c_0^{1/2}} \int_0^\infty \zeta^{-1/2} F_Z(T-\zeta/c_0, X-\zeta, Z)\,\mathrm{d}\zeta \;+\; \text{c.c.} \tag{4.22}$$

This velocity jump is of the same order as that across the critical layer, $J_C^{(3)}$ in (3.26), which incorporates the leading-order linear effect. The scaling (2.31) is thus the 'threshold' amplitude for nonlinear effects to cause a significant departure from linear behaviour.

5. The modulation equation

It follows from (2.27) that the phase shift ϕ is related to the velocity jumps by

$$\phi = \frac{1}{12\lambda_4\alpha_0\hat{c}^3A_0}\left(J_C^{(3)} + J_D^{(3)}\right) \,. \tag{5.1}$$

Substituting this into (2.29), and using (3.26), (4.17), (4.18) and (4.22), we obtain the amplitude equation

$$\frac{\partial P_0}{\partial T} + c_g\frac{\partial P_0}{\partial X} - \mathrm{i}\,d\,\frac{\partial^2 P_0}{\partial Z^2} = \kappa\,P_0 + \mathrm{i}\,\mu P_0 Q \,, \tag{5.2}$$

where

$$Q = \int_0^\infty \zeta^{-1/2}\frac{\partial}{\partial Z}\left(P_0\frac{\partial P_0^*}{\partial Z}\right)(T-\zeta/c_0, X-\zeta, Z)\,\mathrm{d}\zeta \;; \tag{5.3}$$

the coefficients are given by

$$c_g = 2c_0 = 2\left(\omega/\lambda\right)^{1/2} \,, \quad d = (2\lambda)^{-1} \,, \quad \mu = \tfrac{1}{2}\pi^{3/2}\alpha_0 c_0^{3/2}\lambda^{-3} = \tfrac{1}{2}\pi^{3/2}\omega^{5/4}\lambda^{-13/4} \,, \tag{5.4}$$

and $\kappa = \kappa_R + \mathrm{i}\,\kappa_I$, with

$$\kappa_R = \lambda\alpha_0/(2\omega)^{1/2} + 12\pi\lambda_4\alpha_0\hat{c}^4/\lambda^2 = (\lambda^3/2)^{1/2} + 12\pi\lambda_4\omega^{5/2}\lambda^{-15/2} \,. \tag{5.5}$$

Coefficients excepted, this equation is the same as that found by Wu (1993*a*) for the strongly viscous limit of a Rayleigh-wave problem with an unsteady critical layer. We note that the nonlinear term is non-local, and involves the highest-order derivative. In these respects, the amplitude equation (5.2) resembles those found by Smith & Walton (1989) and Hall & Smith (1989) in their studies of wave–vortex interactions close to the lower-branch neutral curve (see also Smith & Blennerhassett 1992). In those studies the dominant mean-flow distortion arises in a wall-buffer layer, which plays an analogous rôle to our diffusion layer. However, because in the aforementioned lower-branch analyses (*a*) the basic flow in the wall-buffer layer is effectively a uniform shear, rather than a uniform velocity, and (*b*) spatially evolving disturbances were studied, the analogous integral to (5.3) had a $\zeta^{-1/3}$, rather than a $\zeta^{-1/2}$, factor. A $\zeta^{-1/2}$

factor occurs if the spatio-temporal instability of lower-branch T-S waves is studied (see Hall & Smith 1990 for the case of temporal instability of PPF).

It is convenient to transform into a frame moving with the group velocity by introducing a retarded time variable

$$\tau = T - X/c_g \,. \tag{5.6}$$

We also make the rescaling

$$\bar{\tau} = \kappa_R \tau \,, \quad \bar{X} = \kappa_R X/c_g \,, \quad \bar{Z} = \left(\kappa_R/d\right)^{1/2} Z \,,$$
$$\bar{P}(\bar{\tau},\bar{X},\bar{Z}) = \left(\frac{\mu^2 c_g}{d^2\kappa_R}\right)^{1/4} \mathrm{e}^{-\mathrm{i}\kappa_I X/c_g}\, P_0(T,X,Z) \,. \tag{5.7}$$

It is implicitly assumed here that the linear growth rate, κ_R, is positive. However, the derivation of the amplitude equation (5.2) remains valid if $\kappa_R < 0$, and the analysis may then describe aspects of bypass transition. We note that the derivation breaks down sufficiently close to the upper-branch neutral curve, i.e. when κ_R is very small (cf. Smith, Brown & Brown 1993).

In terms of the scaled variables (5.7), the amplitude equation (5.2) takes the form

$$\frac{\partial \bar{P}}{\partial \bar{X}} - \mathrm{i}\frac{\partial^2 \bar{P}}{\partial \bar{Z}^2} = \bar{P} + \mathrm{i}\bar{P}\int_0^\infty \bar{\zeta}^{-1/2}\left(\bar{P}(\bar{\tau}-\bar{\zeta},\bar{X}-\bar{\zeta},\bar{Z})\bar{P}^*_{\bar{Z}}(\bar{\tau}-\bar{\zeta},\bar{X}-\bar{\zeta},\bar{Z})\right)_{\bar{Z}} \mathrm{d}\bar{\zeta} \,. \tag{5.8}$$

Thus, in contrast to many other weakly nonlinear analyses of wavepackets, the transformation (5.6) does not eliminate one of the independent variables; an effect of the diffusion layer is to ensure that the phase speed is as relevant as the group velocity.

Equation (5.8) cannot be solved analytically in general. Some simplification is obtained when the spanwise lengthscale is asymptotically large or small compared to (2.5): see Appendix B. In the remainder of this section, however, we are principally concerned with solutions of equation (5.8).

5.1. *A 'sideband' instability*

The amplitude equation (5.8) admits the exact solution

$$\bar{P} = p_0 \mathrm{e}^{(1-\mathrm{i}\bar{\beta}^2)\bar{X}+\mathrm{i}\bar{\beta}\bar{Z}} \,, \tag{5.9}$$

corresponding to a pure plane wave; $\bar{\beta}$ is a measure of the obliqueness of the wave. (A slight obliqueness may occur in experiments if the disturbance generator is not exactly perpendicular to the basic flow.) However, the solution (5.9) is unstable to a secondary 'sideband' instability. To see this we write

$$\bar{P} = \mathrm{e}^{(1-\mathrm{i}\bar{\beta}^2)\bar{X}+\mathrm{i}\bar{\beta}\bar{Z}}\left[p_0 + \tilde{\epsilon}p_+(\bar{X})\mathrm{e}^{\mathrm{i}b\bar{Z}+\mathrm{i}b^2\Omega\bar{T}} + \tilde{\epsilon}p_-(\bar{X})\mathrm{e}^{-\mathrm{i}b\bar{Z}-\mathrm{i}b^2\Omega\bar{T}} + \ldots\right] \,, \tag{5.10}$$

substitute into (5.8), and linearize on the assumption that $\tilde{\epsilon} \ll 1$. The resulting governing equations are

$$\frac{\partial p_+}{\partial \bar{X}} + (\mathrm{i}b^2 + 2\mathrm{i}\bar{\beta}b)p_+ = -\mathrm{i}bp_0^2\mathrm{e}^{2\bar{X}}\int_0^\infty \left[(b-\bar{\beta})p_-^*(\bar{X}-\xi) - \bar{\beta}p_+(\bar{X}-\xi)\right]\frac{\mathrm{e}^{-(2+\mathrm{i}b^2\Omega)\xi}\mathrm{d}\xi}{\xi^{1/2}} \,, \tag{5.11}$$

$$\frac{\partial p_-}{\partial \bar{X}} + (\mathrm{i}b^2 - 2\mathrm{i}\bar{\beta}b)p_- = -\mathrm{i}bp_0^2\mathrm{e}^{2\bar{X}}\int_0^\infty \left[(b+\bar{\beta})p_+^*(\bar{X}-\xi) + \bar{\beta}p_-(\bar{X}-\xi)\right]\frac{\mathrm{e}^{-(2-\mathrm{i}b^2\Omega)\xi}\mathrm{d}\xi}{\xi^{1/2}} \,. \tag{5.12}$$

As a result of the growth of the planar wave, this secondary sideband instability is an *initial-value* problem, in contrast to the more familiar *eigenvalue* problem that arises in the sideband instability of an equilibrium solution (e.g. Stuart & DiPrima 1978), or in certain other 'secondary-instability' theories (e.g. Herbert 1988).

For simplicity, we restrict attention to the stability of a two-dimensional plane wave, i.e. with $\bar{\beta} = 0$. A solution of (5.11) and (5.12) is then sought subject to

$$p_+ \sim \mathrm{e}^{-\mathrm{i}b^2\bar{X}}\,,\quad p_- \to 0 \quad \text{as} \quad \bar{X} \to -\infty\,, \tag{5.13}$$

so that the initial perturbation of the two-dimensional T-S wave is assumed to consist of a single 'sideband' (p_+); the other sideband (p_-) is subsequently generated through nonlinear interactions. The solution may be expressed in series form

$$p_+ = \mathrm{e}^{-\mathrm{i}b^2\bar{X}} \sum_{m=0}^{\infty} p_+^{(m)} \mathrm{e}^{4m\bar{X}}\,,\quad p_- = \mathrm{e}^{\mathrm{i}b^2\bar{X}} \mathrm{e}^{2\bar{X}} \sum_{m=0}^{\infty} p_-^{(m)} \mathrm{e}^{4m\bar{X}} \tag{5.14}$$

(cf. Goldstein & Lee 1992; Wundrow, Hultgren & Goldstein 1994), with coefficients given by

$$\begin{aligned} p_+^{(m)} &= \frac{(-\frac{1}{2} - \frac{1}{2}\mathrm{i}b^2)!}{(m - \frac{1}{2} - \frac{1}{2}\mathrm{i}b^2)!m!} \left\{ \frac{[\frac{1}{2}\mathrm{i}b^2(\Omega-1)]!}{[2m + \frac{1}{2}\mathrm{i}b^2(\Omega-1)]!} \right\}^{1/2} \left(\frac{\pi b^4 |p_0|^4}{32} \right)^m , \\ p_-^{(m)} &= -\frac{\mathrm{i}\pi^{1/2} b^2 p_0^2}{2^{5/2}} \frac{(-\frac{1}{2} + \frac{1}{2}\mathrm{i}b^2)!}{(m + \frac{1}{2} + \frac{1}{2}\mathrm{i}b^2)!m!} \left\{ \frac{[-\frac{1}{2}\mathrm{i}b^2(\Omega-1)]!}{[2m + 1 - \frac{1}{2}\mathrm{i}b^2(\Omega-1)]!} \right\}^{1/2} \left(\frac{\pi b^4 |p_0|^4}{32} \right)^m \end{aligned} \tag{5.15}$$

By application of Laplace's method (Bender & Orszag 1978), we find the large-$\bar{X}$ behaviour

$$\begin{aligned} p_+ &\sim C\mathrm{e}^{-\mathrm{i}b^2\bar{X}} \exp\left[\tfrac{3}{4}\pi^{1/3} b^{4/3} |p_0|^{4/3} \mathrm{e}^{4\bar{X}/3} - 4\sigma\bar{X} \right] , \\ p_- &\sim -\mathrm{i}\mathrm{e}^{2\mathrm{i}\arg(p_0)} C^* \mathrm{e}^{\mathrm{i}b^2\bar{X}} \exp\left[\tfrac{3}{4}\pi^{1/3} b^{4/3} |p_0|^{4/3} \mathrm{e}^{4\bar{X}/3} - 4\sigma^*\bar{X} \right] , \end{aligned} \tag{5.16}$$

with

$$\sigma = \frac{1 + \mathrm{i}b^2(\Omega - 3)}{12}\,, \tag{5.17}$$

$$C = \frac{2^{\mathrm{i}b^2(1-\Omega)/4}}{2.3^{1/2}\pi^{3/4}} \left(-\tfrac{1}{2} - \tfrac{1}{2}\mathrm{i}b^2\right)! \left\{ [\tfrac{1}{2}\mathrm{i}b^2(\Omega-1)]! \right\}^{1/2} \left(\tfrac{1}{64}\pi b^4 |p_0|^4 \right)^{-\sigma} . \tag{5.18}$$

The result (5.16) indicates that the three-dimensional perturbations have an 'exponential of exponential' form of growth because of sideband resonance (cf. Smith 1986; Stewart & Smith 1992; Smith, Stewart & Bowles 1994). This behaviour is similar to that found by Goldstein & Lee (1992), and Wundrow *et al.* (1994), although here the secondary instability involves a pair of *fundamental* oblique modes, whereas they demonstrated the secondary instability of a growing planar wave to a *subharmonic* oblique disturbance (see also Zelman & Maslennikova 1993).

The leading-order growth rate in (5.16) is proportional both to the four-thirds power of the amplitude of the plane wave, and to the four-thirds power of the

spanwise wavenumber b. The latter implies that the 'most unstable' oblique modes will have spanwise wavelengths much shorter than those considered here.† However, for large-b modes, the form (5.16) is only attained at an asymptotically large distance downstream, with $\bar{X} \gg \frac{1}{2}\ln|b|$. Further upstream, or more precisely for

$$\bar{X} \ll \min\left(\tfrac{1}{2}\ln|b|, \tfrac{1}{2}\ln|b(\Omega-1)|\right) , \tag{5.19}$$

an analysis of the series coefficients shows that provided $\Omega \neq 1$, large-b disturbances have the asymptotic behaviour

$$\left.\begin{aligned} p_+ &\sim \mathrm{e}^{-\mathrm{i}b^2\bar{X}} \exp\left[\frac{\pi|p_0|^4}{8(\Omega-1)}\mathrm{e}^{4\bar{X}}\right] , \\ p_- &\sim -\frac{\mathrm{e}^{\mathrm{i}\pi\,\mathrm{sgn}(\Omega-1)/4}\pi^{1/2}p_0^2}{2|b|(|\Omega-1|)^{1/2}}\mathrm{e}^{(2+\mathrm{i}b^2)\bar{X}} \exp\left[\frac{\pi|p_0|^4}{8(\Omega-1)}\mathrm{e}^{4\bar{X}}\right] . \end{aligned}\right\} \tag{5.20}$$

Thus, if $\Omega < 1$, there is a period of superexponential decay before the form (5.16) is attained, while if $\Omega > 1$, (5.20) predicts superexponential growth, but with growth rate independent of b. This implies that the development of the sideband instability depends on the exciting frequency as well as the initial amplitude, and that nonlinear effects may not necessarily be triggered by the large-b modes.

The solution (5.10), (5.14)–(5.15) is illustrated in figure 3 for $b = \pi$, $\Omega = 0$. (The amplitude parameter $\tilde{\epsilon}$ in (5.10), which is formally infinitesimal in the foregoing analysis, has been set equal to 0.0001 for comparison with the full numerical solution of equation (5.8) to be presented in §5.2 below.) The superexponential growth for large $\bar{X}$ given by (5.16) is evident, as is the asymptotic behaviour (5.20) even though b is not especially large.

Finally for this subsection, we note from (5.20) that disturbances with frequencies $\Omega \approx 1$ need special treatment. In order to understand the behaviour in this case, we return to the asymptotic form (5.16), which gives

$$|p_\pm| \sim |C| \exp\left[\tfrac{3}{4}\pi^{1/3}b^{4/3}|p_0|^{4/3}\mathrm{e}^{4\bar{X}/3} - \tfrac{1}{3}\bar{X}\right] , \tag{5.21}$$

with C specified by (5.8). In this terminal régime, the growth-rate is independent of Ω, but for any fixed b, the amplitude $|C|$ is maximized when $\Omega = 1$, and for large b is sharply peaked about this value. This suggests that for a broadband initial disturbance of sufficiently small amplitude, modes with $|b| \gg 1$ and $\Omega \approx 1$ will experience the largest net growth, and so may be the most likely to trigger nonlinearity. For such a mode, with

$$\Omega = 1 + b^{-2}\tilde{\Omega} , \tag{5.22}$$

and $\tilde{\Omega}$ of order one, the transient stage (5.20) has a large superexponential growth (or decay) rate, of $O(b^2\tilde{\Omega}^{-1})$, but is restricted to at most a relatively short range of $\bar{X}$, with $\mathrm{e}^{4\bar{X}} \lesssim O(b^{-2}\tilde{\Omega}^2)$, so that the net growth (or decay) over this phase of development is insignificant compared to that of modes with the same b but Ω not close to 1. However, at somewhat larger distances downstream, with

$$\tfrac{1}{2}\ln|b^{-1}\tilde{\Omega}| \ll \bar{X} \ll \tfrac{1}{2}\ln|b| \tag{5.23}$$

† The absence of a fastest-growing mode makes for difficulties in the numerical solution of (5.8), because of the rapid growth of rounding error. This may be controlled, however, by the use of a 'spectral filter' (cf. Krasny 1986).

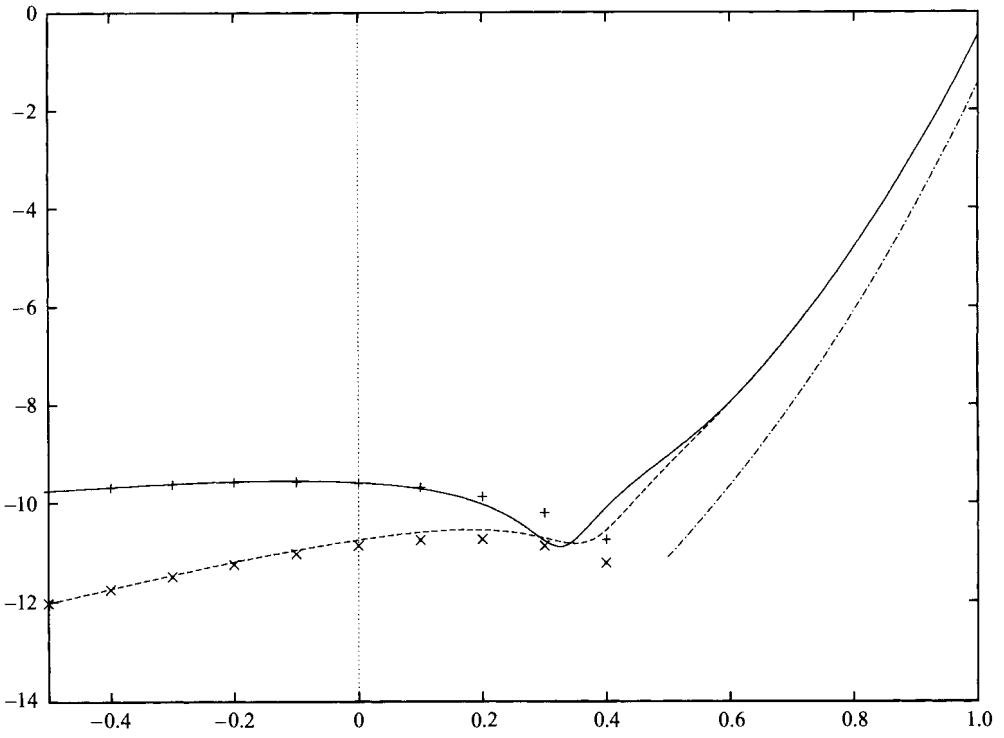

FIGURE 3. The solution (5.14)–(5.15) of the sideband-instability problem (5.10)–(5.13), with $\tilde{\beta} = 0$, $b = \pi$, $\Omega = 0$, $\tilde{\epsilon} = 0.0001$. The abscissa is $\bar{X}$. ——, $\ln(\tilde{\epsilon}^{\bar{X}}|p_+|)$; — — —, $\ln(\tilde{\epsilon}^{\bar{X}}|p_-|)$; +, asymptotic prediction (5.20) for $\ln(\tilde{\epsilon}^{\bar{X}}|p_+|)$; ×, asymptotic prediction (5.20) for $\ln(\tilde{\epsilon}^{\bar{X}}|p_-|)$; — · —, asymptotic prediction (5.16) for $\ln(\tilde{\epsilon}^{\bar{X}}|p_\pm|)$.

we find the asymptotic behaviour

$$p_+ \sim D\mathrm{e}^{-\mathrm{i}b^2\bar{X}} \exp\left[\tfrac{1}{4}(1-\mathrm{i})\pi^{1/2}|b||p_0|^2\mathrm{e}^{2\bar{X}} - \tfrac{1}{2}(1+\mathrm{i}\tilde{\Omega})\bar{X}\right],$$

$$p_- \sim -\frac{\pi^{1/2}p_0^2}{2^{3/2}} D^*\mathrm{e}^{\mathrm{i}b^2\bar{X}} \exp\left[\tfrac{1}{4}(1+\mathrm{i})\pi^{1/2}|b||p_0|^2\mathrm{e}^{2\bar{X}} - \tfrac{1}{2}(1+\mathrm{i}\tilde{\Omega})\bar{X}\right], \tag{5.24}$$

where

$$D = \frac{1}{2^{3/4}\pi^{1/4}} \left[\left(\frac{\mathrm{i}\tilde{\Omega}}{2}\right)!\right]^{1/2} \left[\frac{1}{4}(1-\mathrm{i})\pi^{1/2}|b||p_0|^2\right]^{-(1+\mathrm{i}\tilde{\Omega})/4} \tag{5.25}$$

In this intermediate régime the sidebands grow superexponentially, with growth rate proportional both to the spanwise wavenumber and to the square of the plane-wave amplitude.

The significance of $\Omega \approx 1$ may be understood as follows. In view of (2.4), (2.9) and (5.7), the interaction described by (5.10) and (5.13) starts far upstream with a two-dimensional wave of frequency $\sigma^2\omega$, streamwise wavenumber $\sigma\alpha + O(\sigma^4)$, and wave speed

$$\sigma c_{2D} = \sigma\left(\frac{\omega}{\alpha}\right) + O(\sigma^4), \tag{5.26}$$

perturbed by a three-dimensional sideband for which the corresponding quantities are

$$\left.\begin{aligned} \sigma^2\omega_{3D} &\equiv \sigma^2\omega - \sigma^5 b^2\kappa_R\Omega\,, \\ \sigma\alpha_{3D} &\equiv \sigma\alpha - \sigma^4 b^2\kappa_R(1+\Omega)/c_g + O(\sigma^4)\,, \\ \sigma c_{3D} &\equiv \sigma\left(\omega_{3D}/\alpha_{3D}\right) = \sigma c_{2D} + \sigma^4 b^2\frac{\kappa_R(1-\Omega)}{2\omega} + O(\sigma^4, \sigma^5 b^2, \sigma^8 b^4) \end{aligned}\right\} \tag{5.27}$$

in the limit $|b| \gg 1$ (note that we have used $c_g = 2(\omega/\alpha) + O(\sigma)$ in obtaining the last result). Thus, if $\Omega \neq 1$, the large-b limit involves an increasing discrepancy between the phase speeds of the two- and three-dimensional components, and a consequent separation of their critical levels. A distinguished scaling arises, and the above description fails, when the difference in phase speeds, and thus the separation of the critical levels, is comparable with the critical-layer thickness, namely when

$$\sigma^4 b^2 \sim \sigma^3\,, \quad \text{i.e.} \quad b \sim \sigma^{-1/2}\,. \tag{5.28}$$

Analysis of this new régime (Jennings, Stewart & Wu 1996, in preparation) shows that as $\sigma^{1/2}b$ increases, the interaction of the two-dimensional mode with the sideband is drastically reduced in strength. On the other hand, when $\Omega = 1 + O(b^{-2})$ the two modes have essentially the same critical layer and so can interact more efficiently. Even in this case, however, the present analysis is not valid for arbitrarily large b, since it turns out that when b rises to $O(\sigma^{-3/5})$ a new type of nonlinear ('phase-locked') interaction comes into play. This is discussed in detail by Jennings, Stewart & Wu (1996, in preparation) (see also Wu & Stewart 1996 for analogous work on 'phase-locked' interactions of Rayleigh instability modes in free shear flows).

5.2. *Numerical solutions and a focusing singularity*

Numerical solutions to (5.8) have been obtained on the assumption that $\bar{P}$ is independent of time† and periodic in the spanwise direction, so that

$$\bar{P}(\bar{\tau}, \bar{X}, \bar{Z}) = \sum_{n=-\infty}^{n=\infty} p_n(\bar{X}) \mathrm{e}^{\mathrm{i}nb\bar{Z}}\,, \tag{5.29}$$

where b is the spanwise wavenumber. The Fourier series was suitably truncated, and the solution stepped forward in $\bar{X}$ using a predictor-corrector scheme.

Figures 4 and 5 show the numerical solution for an initial condition consisting of a planar disturbance with a slight periodic distortion in the spanwise direction, namely

$$\bar{P} \sim (1 + \tilde{\epsilon}\,\mathrm{e}^{\mathrm{i}b\bar{Z} - \mathrm{i}b^2\bar{X}})\mathrm{e}^{\bar{X}} \quad \text{as} \quad \bar{X} \to -\infty\,, \tag{5.30}$$

with $b = \pi$ and $\tilde{\epsilon} = 0.0001$. This is the same type of initial condition as in the sideband-instability analysis of the previous section, except that $\tilde{\epsilon}$ is now finite. In fact, the development of the disturbance closely follows the predictions of (5.14)–(5.15) for $\bar{X} \lesssim 0.9$, as can be seen from a comparison of figures 3 and 4. There is a range of $\bar{X}$ over which the three-dimensional component decays, before growing superexponentially further downstream. Moreover, the first-harmonic amplitudes $|p_{\pm 1}|$ tend towards equality, and the disturbance becomes essentially symmetric in $\bar{Z}$. All this is consistent with the asymptotic descriptions (5.20) and (5.16). Subsequently,

† As a referee notes, a purely harmonic dependence could of course be accommodated. However, such a frequency shift could equally well be absorbed into the definition of ω – see the discussion leading up to (2.4).

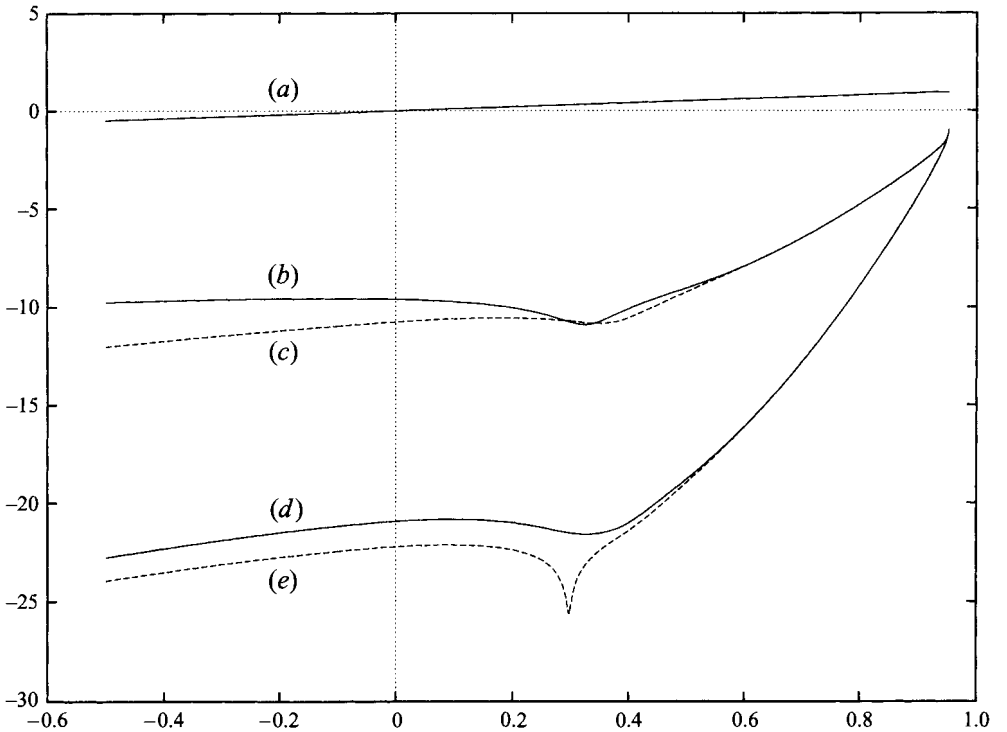

FIGURE 4. A numerical solution to equation (5.8) for the initial condition (5.30); there is no modulation in time. The abscissa is $\bar{X}$. (*a*) $\ln|p_0|$, (*b*) $\ln|p_1|$, (*c*) $\ln|p_{-1}|$, (*d*) $\ln|p_2|$, (*e*) $\ln|p_{-2}|$.

however, the development of the higher harmonics leads to increasing departure from a sinusoidal profile, as shown by figure 5. At this stage, energy is concentrating in the spanwise direction, and it appears that the solution may be approaching a singularity at a finite distance downstream, $\bar{X} = \bar{X}_s$ say, and at a particular spanwise position, $\bar{Z} = \bar{Z}_s$.

Among possible singularity structures, a distinguished case has

$$\bar{P} \sim \frac{\mathrm{e}^{\mathrm{i}\theta} G(\eta)}{(\bar{X}_s - \bar{X})^{1/4 - \mathrm{i}K}} + \dots , \quad \eta = \frac{\bar{Z} - \bar{Z}_s}{(\bar{X}_s - \bar{X})^{1/2}} , \tag{5.31}$$

where K and θ are real parameters. Substitution of (5.31) into (5.8) gives an equation for G, namely

$$\left(\tfrac{1}{4} - \mathrm{i}K\right) G + \tfrac{1}{2}\eta G' - \mathrm{i}G'' = \mathrm{i}G \int_0^\eta \frac{2\xi (G(\xi) G^{*\prime}(\xi))'}{\eta(\eta^2 - \xi^2)^{1/2}} \mathrm{d}\xi . \tag{5.32}$$

Since θ is arbitrary, we can take $G(0)$ to be real and positive. It remains to show that there exist choices of $G(0)$ and K such that a solution to (5.32) exists with

$$G \sim \bar{g} \eta^{-2(1/4 - \mathrm{i}K)} \quad \text{as} \quad |\eta| \to \infty , \tag{5.33}$$

where $\bar{g}$ is a constant. Equation (5.32) was solved numerically. For a given choice of $G(0)$ and K, a series solution was constructed for small η, on the assumption that $G'(0) = 0$. This was then 'marched' to larger values of η using the numerical scheme described in Appendix C. In figure 6 we have plotted $|G(\eta)|$ and $(\arg G)'$ for a solution

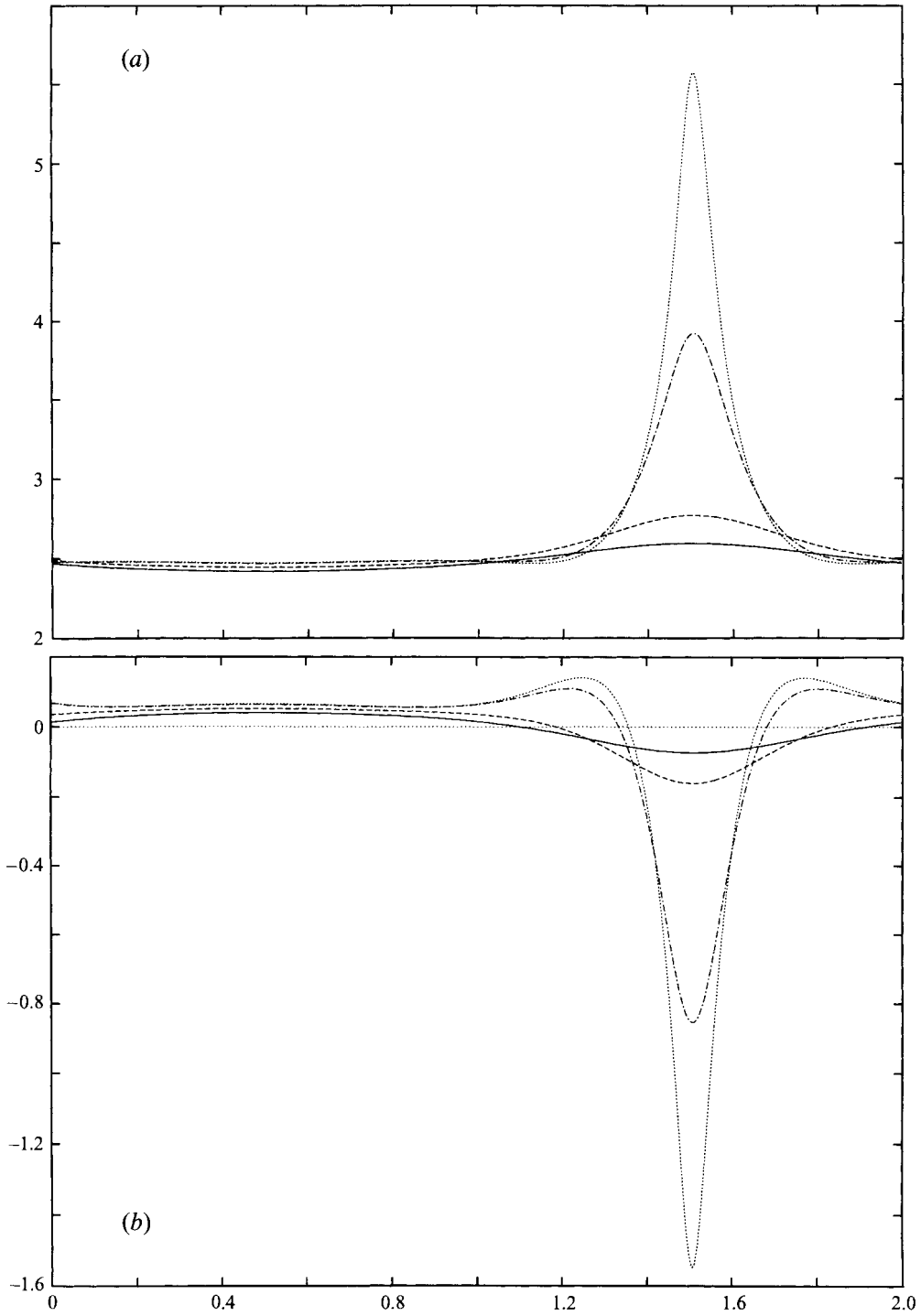

FIGURE 5. The same numerical solution as in figure 4. (*a*) $|\bar{P}|$ *vs.* $\bar{Z}$, (*b*) $\arg \bar{P}$ *vs.* $\bar{Z}$. ——, $\bar{X} = 0.91$; – – –, $\bar{X} = 0.93$; – · –, $\bar{X} = 0.95$; · · ·, $\bar{X} = 0.952$.

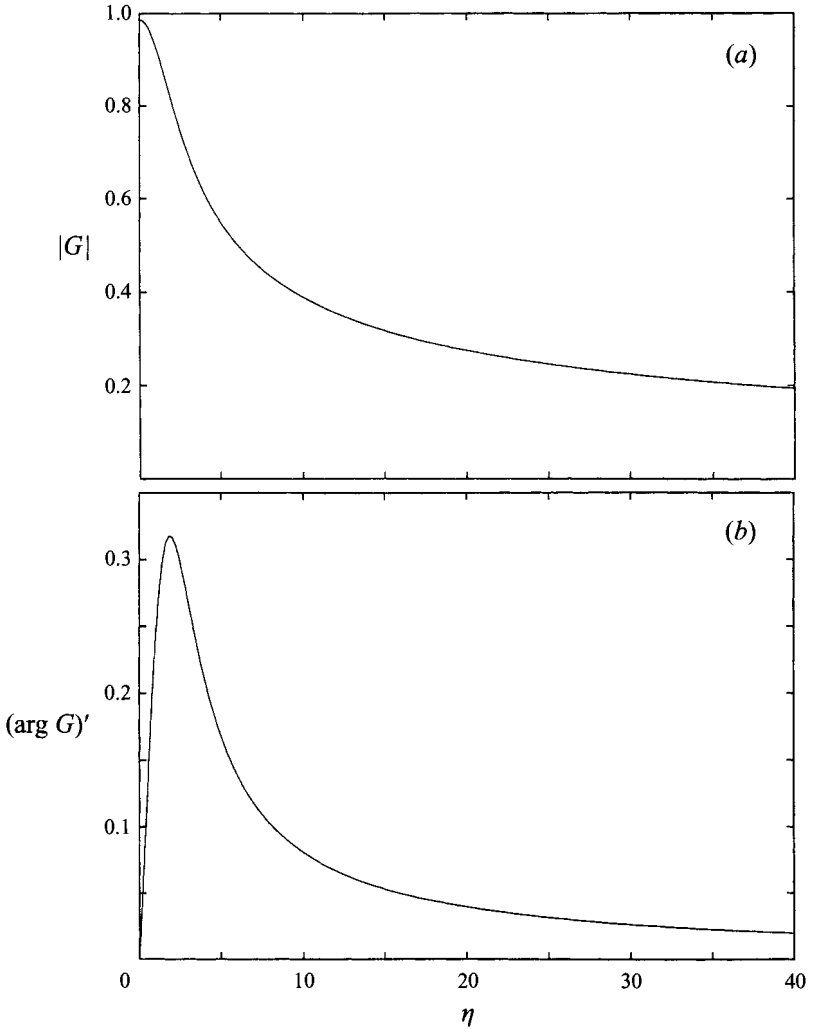

FIGURE 6. A numerical solution to (5.32), (5.33) for $K = 0.392851$ and $G(0) = 0.986440$. Details of the numerical method are given in Appendix C. (*a*) $|G|$ *vs.* η, (*b*) $(\arg G)'$ *vs.* η.

with

$$K \approx 0.3928 \quad \text{and} \quad G(0) \approx 0.9864\,. \tag{5.34}$$

We have been unable to determine whether the roots (5.34) are unique. However, since there is at least one solution it follows that (5.31) is an acceptable singularity structure. In order to compare this asymptotic description of the singularity with our numerical solution of equation (5.8), we note that (5.31) predicts

$$4K \log \bar{P}(\bar{X}, \bar{Z}_s) \sim -\arg \bar{P}(\bar{X}, \bar{Z}_s) \quad \text{as } \bar{X} \to \bar{X}_s^- \,. \tag{5.35}$$

Figure 7 shows a plot of these quantities, taken from the numerical solution, at $\bar{Z} = 1.5078$ (very close to the maximum of $|\bar{P}|$ and $|\arg \bar{P}|$), for $\bar{X}$ between 0.94 and 0.952; K is given by (5.34). It is plausible that the graph is approaching a straight line of slope 1, as predicted.

Solutions to the amplitude equation (5.8) merit further study. In particular, the

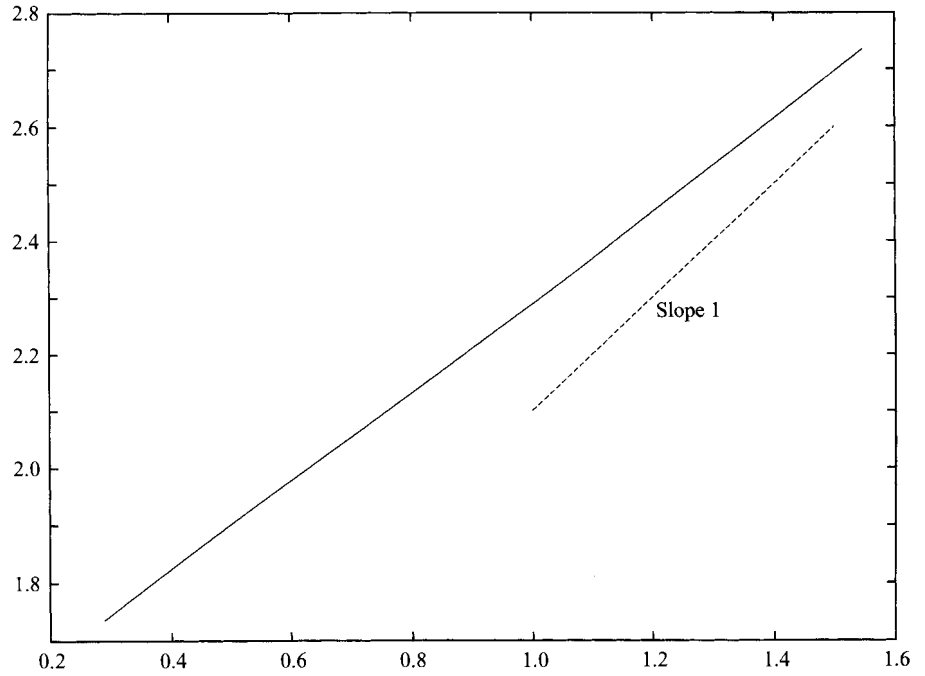

FIGURE 7. A plot of $1.5912 \log|\bar{P}|$ *vs.* $-\arg\bar{P}$ at $\bar{Z} = 1.5078$, for $\bar{X}$ between 0.94 and 0.952, from the numerical solution in figure 5.

inclusion of both temporal and streamwise modulation, and its effect on the formation and structure of singularities, is a matter of current investigation.

5.3. *The next asymptotic stage: a non-equilibrium critical layer induced by the focusing singularity*

In the vicinity of the singularity (5.31), the amplitude equation (5.8) breaks down, and it is therefore necessary to consider a new asymptotic stage. To be specific, (5.31) indicates that close to the singularity $|\bar{P}_{\bar{X}}/\bar{P}| \sim (\bar{X}_s - \bar{X})^{-1}$. Consequently, when

$$\bar{X}_s - \bar{X} = O(\sigma)\,, \tag{5.36}$$

the unscaled (spatial) growth-rate is $O(\sigma^3)$ rather than $O(\sigma^4)$ as in the original scaling (2.4); in other words, the slow growth is now an $O(\sigma^2)$ rather than an $O(\sigma^3)$ correction. For this new scaling, the streamwise-variation term occurs at leading order in the critical-layer equations, so that the critical layer is now of non-equilibrium type. (Wundrow *et al.* 1994 have shown that a similar phenomenon can occur through subharmonic parametric resonance.) It also follows from (5.31) that

$$|\bar{P}_{\bar{Z}}/\bar{P}| \sim (\bar{X}_s - \bar{X})^{-1/2}\,, \tag{5.37}$$

i.e. the spanwise scale shortens. To take account of the evolution over these shorter streamwise and spanwise lengthscales, it is appropriate to introduce

$$\tilde{X} = \sigma^{-1}(\bar{X} - \bar{X}_s)\,, \quad \tilde{Z} = \sigma^{-1/2}(\bar{Z} - \bar{Z}_s)\,. \tag{5.38}$$

In this new asymptotic régime, the (unscaled) magnitude of the disturbance wall-pressure becomes $O(\sigma^{29/4}\sigma^{-1/4}) = O(\sigma^7)$; thus we write

$$\tilde{P}(\tilde{X},\tilde{Z}) = \sigma^{1/4}\bar{P}(\bar{X},\bar{Z})\,. \tag{5.39}$$

We may confirm that for this scaling, cubic interactions within the critical layer can affect the modulation of the disturbance, as follows. The vertical velocity v of the fundamental mode has an $O(\sigma^8)$ magnitude, while its leading-order streamwise (u) and spanwise (w) velocity components in the critical layer are of $O(\sigma^6)$ and $O(\sigma^5)$ respectively. The quadratic interaction of the fundamental with itself, through the vu_y inertia term, drives an $O(\sigma^7)$ streamwise velocity in the form of a mean flow and harmonics. The cubic interaction of these with the fundamental generates an $O(\sigma^8)$ streamwise-velocity correction in the fundamental mode, which balances the $O(\sigma^6\sigma^2)$ spanwise-dispersion term $\partial^2 u/\partial\tilde{Z}^2$. Moreover, the nonlinear interactions within the critical layer occur in the same manner as in Wu (1993*a*). In consequence, the development of the disturbance at this stage is governed by an amplitude equation akin to (5.1) of Wu (1993*a*), namely

$$\frac{\partial\tilde{P}}{\partial\tilde{X}} - \mathrm{i}\frac{\partial^2\tilde{P}}{\partial\tilde{Z}^2} = \mathrm{i}\tilde{\mu}\int_0^\infty\int_0^\infty \mathrm{e}^{-\tilde{s}(2\xi^3+3\xi^2\eta)} \times\Big\{\ \xi^3\ \tilde{P}(\tilde{X}-\xi)\tilde{P}(\tilde{X}-\xi-\eta)\tilde{P}^*_{\tilde{Z}\tilde{Z}}(\tilde{X}-2\xi-\eta) + \xi^2\eta\ \tilde{P}(\tilde{X}-\xi)[\tilde{P}(\tilde{X}-\xi-\eta)\tilde{P}^*_{\tilde{Z}}(\tilde{X}-2\xi-\eta)]_{\tilde{Z}} + \xi^3\ [\tilde{P}(\tilde{X}-\xi)\tilde{P}(\tilde{X}-\xi-\eta)\tilde{P}^*_{\tilde{Z}}(\tilde{X}-2\xi-\eta)]_{\tilde{Z}}\ \Big\}\,\mathrm{d}\xi\,\mathrm{d}\eta\ , \quad (5.40)$$

with

$$\tilde{s} = \tfrac{1}{3}\alpha_0^2\lambda^2\left(\frac{c_g}{\kappa_R c_0}\right)^3\ , \quad \tilde{\mu} = 12\left(\frac{3\tilde{s}^3}{\pi}\right)^{1/2}\ . \quad (5.41)$$

The term proportional to $\tilde{P}$ does not appear in the amplitude equation since the disturbance now evolves over a much faster spatial scale than in the linear growth régime. The appropriate initial condition for this equation follows from matching to the previous stage, i.e. as $\tilde{X}\to-\infty$ we require from (5.31)

$$\tilde{P}\sim(-\tilde{X})^{-1/4+\mathrm{i}K}\mathrm{e}^{\mathrm{i}\theta}G\left(\tilde{Z}/(-\tilde{X})^{1/2}\right)\ . \quad (5.42)$$

It would be interesting to see whether solutions of equation (5.40) with such an initial condition can display the splitting of wavepackets observed by Gaster & Grant (1975).

6. Discussion and conclusions

In this paper we have developed a self-consistent theory to describe the nonlinear evolution of spanwise-modulated T-S wavetrains in boundary layers. In the case of a fixed-frequency disturbance propagating downstream, we have assumed that nonlinearity first becomes significant at streamwise locations in the so-called upper-branch régime. The scale of the spanwise modulation has been fixed by requiring that spanwise dispersion is significant on the slow streamwise-growth scale, while the amplitude of the disturbance has been chosen so that weakly nonlinear effects are also significant on this scale. We find that the dominant nonlinear effects come from the critical layer and the surrounding diffusion layer, in the form of a wave–vortex interaction (cf. Smith & Walton 1989; Wu 1993*a*,*b*; Wu *et al.* 1993; Mankbadi *et al.* 1993; Brown *et al.* 1993; Smith *et al.* 1993). It follows that the evolution of the wavetrain amplitude is governed by an integro-partial-differential equation with a non-local nonlinear term.

We have examined properties of the amplitude equation (5.8) analytically and numerically. Plane T-S waves have been shown to be linearly unstable to a rapidly growing secondary instability of sideband type. Moreover, for the full nonlinear equation we have shown that spanwise modulation can lead to the occurrence of a singularity at a finite distance downstream and at a particular spanwise location. The concentration of energy in the spanwise direction is possibly consistent with the observations of Klebanoff *et al.* (1962) on the formation of streamwise 'streaks'. The formation of the singularity indicates that the wavetrain enters a new stage of development in which the evolution takes place on shorter streamwise and spanwise lengthscales. A close examination shows that, in this new stage, the critical layer is of non-equilibrium type (cf. Wu 1993*a*). A firm comparison with experiments awaits a study of this new asymptotic stage. However, we note that since our analysis is valid for any combination of temporal and streamwise modulation, a direct comparison with experiment may eventually prove possible.† (On the other hand, the recent paper of Healey (1995) suggests that in order to obtain a quantitative comparison, some form of composite, or recast, expansion will probably be necessary). For the scalings in this paper, a study of the effect of simultaneous temporal and streamwise modulation on both the numerical results and the singularity is underway.

Although our analysis is presented for the upper-branch régime, the same evolution equation also applies to the 'high-frequency' limit of the lower-branch régime, provided that the second term in the linear growth rate, κ_R, in (5.5) is dropped (and κ_I suitably modified). In this sense, the upper-branch scaling can be regarded as more general than the HFLB. The weakly nonlinear evolution of spanwise-modulated planar T-S waves in the latter régime has been studied by Stewart & Smith (1992) for boundary layers. Like us, they assumed that spanwise dispersion was comparable with the slow streamwise growth. However, in fixing the nonlinear scaling, they assumed that the critical layer is 'passive' (i.e. the velocity jump is zero). Our analysis suggests that this assumption is questionable. Indeed we find that, for our scaling, the critical layer and diffusion layer are the most active regions as far as the nonlinear dynamics are concerned. Specifically, for our choice of disturbance amplitude, the nonlinear term in (5.3) arises from a wave–vortex interaction within these layers, while nonlinearity in the bulk of the flow is a higher-order effect.

Likewise, in the analogous problem for PPF, because of the sensitivity to nonlinearity of the critical layer and the accompanying diffusion layer, nonlinear effects actually come into play at much lower amplitudes than those considered by Smith & Bowles (1992), who again assume a 'passive' critical layer. An analysis of PPF from the perspective of our amplitude equation is given by Stewart & Wu (1996, in preparation).

The related work of Smith & Stewart (1987), concerning 'resonant-triad' interactions in the HFLB régime of a boundary layer, also assumes no velocity jump across the critical layer (see also Bassom & Hall 1991). Again, we feel that this assumption needs further justification.‡ Indeed, Mankbadi *et al.* (1993) and Wu (1993*b*) have studied resonant-triad interactions of T-S waves with the upper-branch scaling for both the Blasius boundary layer and boundary layers with pressure gradients (see also Mankbadi 1991). In both cases, a diffusion layer exists and the total velocity jump across the critical layer and diffusion layer is non-zero. Moreover, Jennings *et al.* (1996, in preparation) have explicitly confirmed that the resonant-triad equations of

† Stewart & Smith (1992) compared a spatio-temporal theory, which was not valid in the purely spatial case, with spatial experiments. See also later comments.

‡ This point has also been made by Khokhlov (1991, 1993).

Mankbadi *et al.* (1993) and Wu (1993*b*) can be derived in the HFLB limit (as was to be expected), with nonlinear interactions becoming significant at smaller disturbance amplitudes than those considered by Smith & Stewart (1987). In addition, Jennings *et al.* (1996, in preparation) find solutions involving both spanwise and streamwise modulation.

In the light of the above we believe that, especially in the case of three-dimensional disturbances, there is no *a priori* reason for assuming that the velocity jump across a critical level is zero. Furthermore, in a viscous fluid, a diffusion layer will in general develop, and this layer can crucially affect the velocity jump. A consequence of this is that the velocity jump across a 'steady' critical level can differ from the velocity jump across an evolving critical level, even when an inner critical layer in the latter case has achieved a quasi-steady state (which may be asymptotically inviscid): see for example Cowley (1981), Haynes & Cowley (1986), Gajjar & Smith (1985). We believe, therefore, that in the case of a real viscous fluid, a careful justification is required if a detailed study of (critical layers and) diffusion layers is to be avoided in any predominantly inviscid, time-dependent, nonlinear analysis (e.g. that of Smith 1992). Indeed, such justification is particularly important in inviscid analyses where viscous diffusion is (implicitly) invoked to ensure that the vorticity distribution within the 'cats-eyes' does not have a (pathological) small-scale structure (cf. Stewartson 1978; Brown & Stewartson 1978; Goldstein & Hultgren 1988).

The authors would like to thank Mr M. J. Jennings for assistance with the computations, especially those described in Appendix C, and Professor J. T. Stuart FRS for his helpful comments. Part of this work was carried out while X.W. and S.J.C. were visiting NASA Lewis Research Centre in August 1992. Discussions with Dr M. E. Goldstein and Dr S. S. Lee during this period are gratefully acknowledged. Thanks are also due to the referees for their helpful comments, and for pointing out a number of typographical errors in an earlier version of the manuscript. The computations were supported by a Royal Society Research Grant and the SERC 'Computational Science Initiative' Grant GR/H57585. This work was presented at the International Workshop on Advances in Analytical Methods in Aerodynamics, 12-14 July 1993, Miedzyzdroje, Poland.

Appendix A. The 'high-frequency' lower-branch régime

As indicated in §1, at least as far as linear theory is concerned, the so-called 'high-frequency' lower-branch (HFLB) régime is equivalent, in our terminology, to the 'upstream' limit of the upper-branch régime. The aim of this Appendix is to demonstrate that this is still so in the case of our weakly nonlinear theory.

The lower-branch régime for an incompressible boundary layer (with or without pressure gradient) is described by a 'triple-deck' structure (Smith 1979, 1986; Smith & Stewart 1987). The relevant scalings for the horizontal coordinates and time are

$$\hat{X} = R^{-1/4}x\,, \quad \bar{X} = R^{-1}x\,, \quad \hat{Z} = R^{-1/4}z\,, \quad \hat{T} = R^{-1/2}t\,. \tag{A 1}$$

In the main part of the boundary layer (the 'middle deck'), the flow perturbation is effectively inviscid; viscous effects are only significant in a sublayer (the 'lower deck') where the appropriate normal coordinate is

$$\hat{Y} = R^{1/4}y\,, \tag{A 2}$$

and the velocity components and pressure scale as

$$\hat{U} = R^{1/4}u\,, \quad \hat{V} = R^{3/4}v\,, \quad \hat{W} = R^{1/4}w\,, \quad \hat{\mathscr{P}} = R^{1/2}p\,. \tag{A 3}$$

The governing equations for the lower deck are then

$$\hat{U}_{\hat{X}} + \hat{V}_{\hat{Y}} + \hat{W}_{\hat{Z}} = 0, \tag{A 4}$$

$$\hat{U}_{\hat{T}} + \hat{U}\hat{U}_{\hat{X}} + \hat{V}\hat{U}_{\hat{Y}} + \hat{W}\hat{U}_{\hat{Z}} = -\hat{\mathscr{P}}_{\hat{X}} + \hat{U}_{\hat{Y}\hat{Y}}\,, \tag{A 5}$$

$$\hat{W}_{\hat{T}} + \hat{U}\hat{W}_{\hat{X}} + \hat{V}\hat{W}_{\hat{Y}} + \hat{W}\hat{W}_{\hat{Z}} = -\hat{\mathscr{P}}_{\hat{Z}} + \hat{W}_{\hat{Y}\hat{Y}}\,, \tag{A 6}$$

$$\hat{\mathscr{P}}_{\hat{Y}} = 0, \tag{A 7}$$

with the wall-boundary condition

$$\hat{U} = \hat{V} = \hat{W} = 0 \quad \text{on} \quad \hat{Y} = 0. \tag{A 8}$$

The leading-order solution in the 'middle deck' provides the outer boundary condition on (A 4)–(A 5), namely

$$\hat{U} \sim \Lambda(\bar{X})(\hat{Y} + \mathscr{A}), \ \hat{W} \to 0 \quad \text{as} \quad \hat{Y} \to \infty, \tag{A 9}$$

while that in the 'upper deck' (outside the boundary layer) gives the 'interaction' relation

$$\hat{\mathscr{P}} = -\frac{1}{2\pi}\int_{-\infty}^{\infty}\int_{-\infty}^{\infty} \frac{\mathscr{A}_{\hat{X}'\hat{X}'}}{\left[(\hat{X}-\hat{X}')^2 + (\hat{Z}-\hat{Z}')^2\right]^{1/2}} \mathrm{d}\hat{X}'\mathrm{d}\hat{Z}'\,, \tag{A 10}$$

between the (unknown) functions $\mathscr{A}(\hat{T},\hat{X},\hat{Z};\bar{X})$ and $\hat{\mathscr{P}}(\hat{T},\hat{X},\hat{Z};\bar{X})$. Finally, if the flow perturbation vanishes far upstream,

$$\hat{U} \sim \Lambda(\bar{X})\hat{Y} \quad \text{as} \quad \hat{X} \to -\infty. \tag{A 11}$$

$\Lambda(\bar{X})$ is the local undisturbed wall shear. For a fixed-frequency disturbance, the far-downstream limit of the lower-branch régime corresponds to $\Lambda(\bar{X}) \to 0$. Linear solutions in this limit can be shown to match to upper-branch solutions in the 'upstream' limit. However, $\Lambda(\bar{X})$ can be scaled from the problem, i.e. without loss of generality $\Lambda(\bar{X}) = 1$. Mathematically, the far-downstream limit then corresponds to the 'high-frequency' limit of Zhuk & Ryzhov (1982) and Smith & Burggraf (1985). In order to spell out the link between our upper-branch approach and the HFLB, we here outline a derivation of (5.8) from the standpoint of a HFLB limit.

We assume that the disturbance has a given fixed frequency, $\hat{\Omega}$, and that

$$\hat{\Omega} \gg 1\,. \tag{A 12}$$

From the properties of the linear solution (Zhuk & Ryzhov 1982; Smith & Burggraf 1985; Stewart & Smith 1992), it is known that appropriate scalings for the time and horizontal coordinates are

$$\hat{T} = \hat{\Omega}^{-1}t = T\,, \quad \hat{X} = \hat{\Omega}^{-1/2}x = \hat{\Omega}^{1/2}X\,, \quad \hat{Z} = Z\,. \tag{A 13}$$

The scalings (A 13) lead to the multiple-scale substitutions

$$\frac{\partial}{\partial\hat{T}} \to \hat{\Omega}\frac{\partial}{\partial t} + \frac{\partial}{\partial T}\,, \quad \frac{\partial}{\partial\hat{X}} \to \hat{\Omega}^{1/2}\frac{\partial}{\partial x} + \hat{\Omega}^{-1/2}\frac{\partial}{\partial X}\,, \quad \frac{\partial}{\partial\hat{Z}} \to \frac{\partial}{\partial Z}\,. \tag{A 14}$$

Arguments similar to those given in the main text, and by Wu (1993*a*), show that in the high-frequency limit, the lower-deck region, i.e. $\hat{Y} = O(1)$, splits into five asymptotic zones, namely

(*a*) a Tollmien layer of width $O(\hat{\Omega}^{1/2})$,
(*b*) a viscous critical layer of width $O(\hat{\Omega}^{-1/6})$,
(*c*) a diffusion layer of width $O(1)$ surrounding the critical layer,
(*d*) a passive wall-buffer layer, of width $O(\hat{\Omega}^{1/6})$ in the case of a purely spatial stability analysis (i.e. with $\partial/\partial T = 0$), but of width $O(1)$ otherwise (e.g. for a temporal stability analysis or a wavepacket analysis), and
(*e*) a viscous Stokes layer of width $O(\hat{\Omega}^{-1/2})$.

A scaling argument based on the analysis in the main text suggests that, for the scalings (A 13), the smallest pressure perturbation which will give rise to a weakly nonlinear response has $\mathscr{P} = O(\hat{\Omega}^{-3/4})$. This is much smaller than the pressure perturbation considered by Stewart & Smith (1992). We therefore write

$$\mathscr{P} = \hat{\Omega}^{-3/4}(\mathscr{P}_0 + \hat{\Omega}^{-1}\mathscr{P}_3 + \ldots)E + \text{c.c.} + \ldots\,, \tag{A 15}$$

$$\mathscr{A} = \hat{\Omega}^{-5/4}(\mathscr{A}_0 + \hat{\Omega}^{-1}\mathscr{A}_3 + \ldots)E + \text{c.c.} + \ldots\,, \tag{A 16}$$

where

$$E = \exp(\mathrm{i}\alpha_0 x - \mathrm{i}t) \quad \text{and} \quad \mathscr{P}_0 = \mathscr{P}_0(T, X, Z)\,, \text{etc.} \tag{A 17}$$

Solutions can now be sought in each of the five asymptotic regions.

(*a*) In the *Tollmien layer*, we put

$$\hat{Y} = \hat{\Omega}^{1/2} Y\,, \tag{A 18}$$

and the expansions corresponding to (A 15) and (A 16) are

$$\hat{U} = \hat{\Omega}^{1/2} Y + \hat{\Omega}^{-5/4}(U_0 + \hat{\Omega}^{-1}U_3 + \ldots)E + \text{c.c.} + \ldots\,, \tag{A 19}$$

$$\hat{V} = \hat{\Omega}^{-1/4}(V_0 + \hat{\Omega}^{-1}V_3 + \ldots)E + \text{c.c.} + \ldots\,, \tag{A 20}$$

$$\hat{W} = \hat{\Omega}^{-7/4}(W_0 + \ldots)E + \text{c.c.} + \ldots\,. \tag{A 21}$$

Solutions can be found in the form

$$U_0 = \mathscr{A}_0\,, \quad V_0 = -\mathrm{i}\alpha_0 \mathscr{A}_0 Y\,, \quad W_0 = \frac{\mathrm{i}}{(\alpha_0 Y - 1)}\frac{\partial \mathscr{P}_0}{\partial Z}\,; \tag{A 22}$$

$$\left.\begin{aligned} U_3 &= a_3^{\pm}(T,X,Z) + \frac{\mathrm{i}}{\alpha_0}\frac{\partial \mathscr{A}_0}{\partial X} - \frac{1}{\alpha_0(\alpha_0 Y - 1)}\frac{\partial^2 \mathscr{P}_0}{\partial Z^2} \qquad (\text{A 23})\\ V_3 &= -\mathrm{i}a_3^{\pm}(\alpha_0 Y - 1) + b_3(T,X,Z) \qquad (\text{A 24}) \end{aligned}\right\} \text{in } Y \gtrless \alpha_0^{-1},$$

where

$$a_3^{+} = \mathscr{A}_3 - \frac{\mathrm{i}}{\alpha_0}\frac{\partial \mathscr{A}_0}{\partial X}\,, \tag{A 25}$$

$$b_3 = -\mathrm{i}\alpha_0 \mathscr{P}_3 - \left(\frac{\partial}{\partial T} + \alpha_0^{-1}\frac{\partial}{\partial X}\right)\mathscr{A}_0 - \frac{\partial \mathscr{P}_0}{\partial X} + \frac{\mathrm{i}}{\alpha_0}\frac{\partial^2 \mathscr{P}_0}{\partial Z^2}\,, \tag{A 26}$$

and a_3^{-} is undetermined at this stage.

(*b*) In the *Stokes layer*, where

$$\hat{Y} = \hat{\Omega}^{-1/2}\check{Y} \tag{A 27}$$

the velocity components expand in the form

$$U = \hat{\Omega}^{-1/2}\check{Y} + \hat{\Omega}^{-5/4}(\check{U}_0 + \ldots)E + \text{c.c.} + \ldots\,, \tag{A 28}$$

$$V = \hat{\Omega}^{-5/4}(\check{V}_0 + \ldots)E + \text{c.c.} + \ldots\,, \quad W = \hat{\Omega}^{-7/4}(\check{W}_0 + \ldots)E + \text{c.c.} + \ldots\,, \tag{A 29}$$

with solutions

$$\check{U}_0 = \alpha_0 \mathscr{P}_0 (1 - \mathrm{e}^{m\check{Y}}) , \tag{A 30}$$

$$\check{V}_0 = -\mathrm{i}\alpha_0^2 \mathscr{P}_0 (\check{Y} - m^{-1}\mathrm{e}^{m\check{Y}} + m^{-1}) , \quad \text{etc.} , \tag{A 31}$$

where $m = \exp \frac{3}{4}\pi \mathrm{i}$.

(*c*) In the *critical layer*, a transverse variable is defined by

$$\hat{Y} - \hat{\Omega}^{\frac{1}{2}}\alpha_0^{-1} = \hat{\Omega}^{-1/6}\eta , \tag{A 32}$$

and the appropriate expansions are

$$\begin{aligned} U = {} & \hat{\Omega}^{1/2}\alpha_0^{-1} + \hat{\Omega}^{-1/6}\eta \\ & + \hat{\Omega}^{-5/4}\left\{(\bar{U}_0 + \hat{\Omega}^{-1/3}\bar{U}_1 + \hat{\Omega}^{-2/3}\bar{U}_2 + \hat{\Omega}^{-5/6}\bar{U}_{5/2} + \hat{\Omega}^{-1}\bar{U}_3 + \ldots)E + \text{c.c.}\right\} \\ & + \hat{\Omega}^{-3/2}\bar{U}_M^{(0)} + \hat{\Omega}^{-5/3}\bar{U}_M^{(1)} + \hat{\Omega}^{-11/6}\bar{U}_M^{(2)} - \tfrac{1}{3}\hat{\Omega}^{-2}\ln\hat{\Omega}\,\bar{U}_M^{(3L)} \\ & + \hat{\Omega}^{-2}\bar{U}_M^{(3)} + \ldots , \end{aligned} \tag{A 33}$$

$$\begin{aligned} V = {} & \hat{\Omega}^{-1/4}(-\mathrm{i}\mathscr{A}_0 + \hat{\Omega}^{-2/3}\bar{V}_0 + \ldots + \hat{\Omega}^{-5/3}\bar{V}_3 + \ldots)E + \text{c.c.} \\ & + \hat{\Omega}^{-3/2}\bar{V}_M^{(2)} - \tfrac{1}{3}\hat{\Omega}^{-5/3}\ln\hat{\Omega}\,\bar{V}_M^{(3L)} + \hat{\Omega}^{-5/3}\bar{V}_M^{(3)} + \ldots , \end{aligned} \tag{A 34}$$

$$W = \hat{\Omega}^{-13/12}(\bar{W}_0 + \ldots)E + \text{c.c.} - \tfrac{1}{3}\hat{\Omega}^{-3/2}\ln\hat{\Omega}\,\bar{W}_M^{(3L)} + \hat{\Omega}^{-3/2}\bar{W}_M^{(3)} + \ldots . \tag{A 35}$$

(*d*) In the *diffusion layer*, likewise

$$\hat{Y} - \hat{\Omega}^{1/2}\alpha_0^{-1} = \tilde{\eta} , \tag{A 36}$$

and

$$\begin{aligned} \tilde{U} = {} & \hat{\Omega}^{1/2}\alpha_0^{-1} + \tilde{\eta} + \hat{\Omega}^{-5/4}\left\{(\tilde{U}_0 + \hat{\Omega}^{-1/2}\tilde{U}_{3/2} + \hat{\Omega}^{-1}\tilde{U}_3 + \ldots)E + \text{c.c.}\right\} \\ & + \hat{\Omega}^{-3/2}\tilde{U}_M + \ldots , \end{aligned} \tag{A 37}$$

$$\begin{aligned} V = {} & \hat{\Omega}^{-1/4}(-\mathrm{i}\mathscr{A}_0 + \hat{\Omega}^{-1/2}\tilde{V}_0 + \ldots + \hat{\Omega}^{-3/2}\tilde{V}_3 + \ldots)E + \text{c.c.} \\ & + \hat{\Omega}^{-3/2}\tilde{V}_M + \ldots , \end{aligned} \tag{A 38}$$

$$W = \hat{\Omega}^{-5/4}(\tilde{W}_0 + \ldots)E + \text{c.c.} + \hat{\Omega}^{-3/2}\tilde{W}_M + \ldots . \tag{A 39}$$

The solutions in the critical layer and diffusion layer can be obtained directly from those in the main text by setting

$$\lambda = 1 , \quad \lambda_4 = 0 , \quad \omega = 1 , \quad c_0 = \hat{c} = \alpha_0^{-1} , \tag{A 40}$$

$$\alpha_i = 0 , \quad c_i = 0 , \quad A_i = 0 \quad \text{for } i = 1, 2, 3L . \tag{A 41}$$

Hence, from (3.26), (4.17). (4.18) and (4.22), the jump in $\partial V_3/\partial Y$ is given by

$$J_3 \equiv -\mathrm{i}\,\alpha_0(a_3^+ - a_3^-) = \tfrac{1}{2}\mathrm{i}\pi^{3/2}\alpha_0^{1/2}\mathscr{A}_0 \int_0^\infty \zeta^{-1/2}\frac{\partial}{\partial Z}\left(\mathscr{P}_0\frac{\partial \mathscr{P}_0^*}{\partial Z}\right)(T - \alpha_0\zeta, X - \zeta, Z)\,\mathrm{d}\zeta . \tag{A 42}$$

Matching the solutions in the Tollmien layer to those in the Stokes layer, and making use of (A 25) and (A 42), we find that

$$\mathscr{A}_0 = \alpha_0 \mathscr{P}_0 , \tag{A 43}$$

$$\mathscr{A}_3 = \alpha_0\mathscr{P}_3 - \mathrm{i}\frac{\partial \mathscr{P}_0}{\partial X} - \frac{1}{\alpha_0}\frac{\partial^2 \mathscr{P}_0}{\partial Z^2} + \exp\left(\frac{\mathrm{i}\pi}{4}\right)\alpha_0^2\mathscr{P}_0 - \mathrm{i}\frac{\partial \mathscr{A}_0}{\partial T} + \frac{\mathrm{i}}{\alpha_0}J_3 . \tag{A 44}$$

The interaction law (A 10) provides the additional relationships

$$\mathscr{P}_0 = \alpha_0 \mathscr{A}_0 \,, \tag{A 45}$$

$$\mathscr{P}_3 = \alpha_0 \mathscr{A}_3 - 2\mathrm{i}\frac{\partial \mathscr{A}_0}{\partial X} + \frac{\mathrm{i}}{\alpha_0}\frac{\partial \mathscr{P}_0}{\partial X} + \frac{1}{2\alpha_0^2}\frac{\partial^2 \mathscr{P}_0}{\partial Z^2} \,. \tag{A 46}$$

Equations (A 43) and (A 45) give

$$\alpha_0 = 1 \,, \tag{A 47}$$

while combination of (A 42), (A 44), and (A 46), and use of (A 45) and (A 47), yields the amplitude-evolution equation

$$\frac{\partial \mathscr{P}_0}{\partial T} + 2\frac{\partial \mathscr{P}_0}{\partial X} - \frac{\mathrm{i}}{2}\frac{\partial^2 \mathscr{P}_0}{\partial Z^2} = \left(\frac{1-\mathrm{i}}{2^{1/2}}\right)\mathscr{P}_0 + \frac{\mathrm{i}\pi^{3/2}}{2}\mathscr{P}_0 \mathscr{Q} \,, \tag{A 48}$$

$$\mathscr{Q} = \int_0^\infty \zeta^{-1/2}\frac{\partial}{\partial Z}\left\{\mathscr{P}_0(T-\zeta, X-\zeta, Z)\frac{\partial \mathscr{P}_0^*}{\partial Z}(T-\zeta, X-\zeta, Z)\right\} \mathrm{d}\zeta \,. \tag{A 49}$$

After the transformation corresponding to (5.6) and (5.7), this equation reduces to the form (5.8).

Appendix B. Limiting cases of the amplitude equation

If the scale of the the spanwise variations differs (slightly) from that assumed in (2.5), namely $z = O(\sigma^{-5/2})$, the amplitude equation (5.2) simplifies. In this Appendix, we examine spanwise variations that are less and more rapid than (2.5).

B.1. *Weak spanwise variations*

In order to examine the case of weak spanwise variations we introduce

$$\hat{Z} = \beta \bar{Z} \,, \quad \hat{P}(\bar{T}, \bar{X}, \hat{Z}) = \beta \bar{P}(\bar{T}, \bar{X}, \bar{Z}) \,, \tag{B 1}$$

where $\beta \ll 1$, and both $\hat{Z}$ and $\hat{P}$ are assumed to be of order one. On substituting (B 1) into (5.8), and then taking the limit $\hat{\beta} \to 0$, we find that $\hat{P}$ is governed, to leading order, by

$$\frac{\partial \hat{P}}{\partial \bar{X}} = \hat{P} + \mathrm{i}\hat{P}\int_0^\infty \zeta^{-1/2}\left(\hat{P}(\bar{T}-\zeta, \bar{X}-\zeta, \hat{Z})\hat{P}_{\hat{Z}}^*(\bar{T}-\zeta, \bar{X}-\zeta, \hat{Z})\right)_{\hat{Z}} \mathrm{d}\zeta \,. \tag{B 2}$$

The unscaled magnitude of the streamwise perturbation velocity in the bulk of the boundary layer is now $O(\sigma^{25/4}\beta^{-1})$. This indicates that for weak spanwise variations, a larger magnitude is needed in order for the nonlinearity to come into play (see also (5.16)).

We do not study the properties of equation (B 2) in depth. It is readily shown, however, that as for the full equation (5.8), plane-wave solutions of (B 2) are subject to sideband instability. Further, preliminary numerical solutions of (B 2), with $\hat{P}$ independent of $\bar{T}$, indicate the emergence of 'spikes' in the amplitude at particular spanwise positions. Unfortunately it is not clear whether the solutions terminate in a singularity. However, we note that a candidate structure for a 'focusing' singularity at a finite distance downstream, $\bar{X} = \bar{X}_s$ say, and a particular spanwise position, $\hat{Z} = \hat{Z}_s$, has the form

$$\hat{P} \sim \nu\left(\sigma - \tfrac{4}{3}\ln\sigma + \tfrac{4}{3}F(\hat{\eta}) + \ldots\right)^{1-\mathrm{i}} \,, \tag{B 3}$$

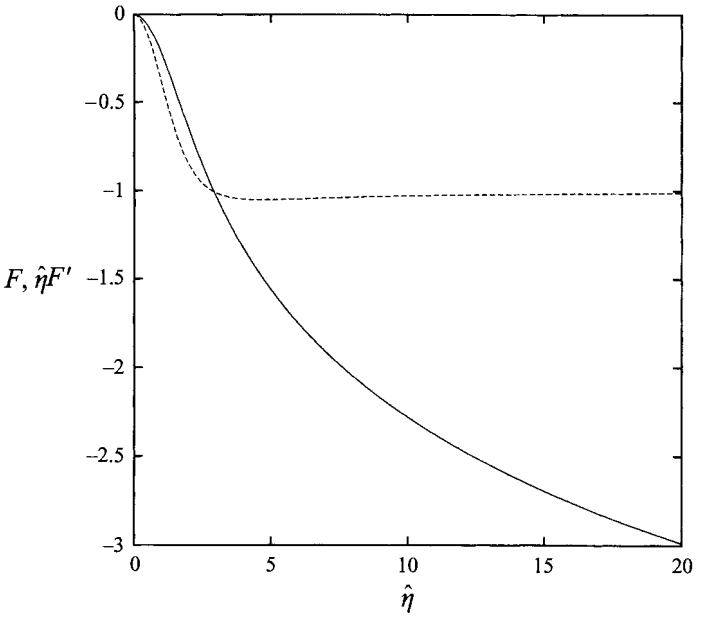

FIGURE 8. The numerical solution to (B 5) with $F(0) = 0$ and $F'(0) = 0$. ——, $F(\hat{\eta})$; – – –, $\hat{\eta}F'(\hat{\eta})$.

where

$$\sigma = \ln(\bar{X}_s - \bar{X})^{-1}\,, \quad \hat{\eta} = \frac{\hat{Z} - \hat{Z}_s}{|v|(\bar{X}_s - \bar{X})^{3/4}\sigma}\,, \tag{B 4}$$

v is an arbitrary complex constant, and $F(\hat{\eta})$ satisfies

$$1 + \hat{\eta}F' = -\int_0^{\hat{\eta}} \frac{16\xi^{1/3}F''(\xi)}{9\hat{\eta}^{2/3}(\hat{\eta}^{4/3} - \xi^{4/3})^{1/2}}\mathrm{d}\xi\,. \tag{B 5}$$

On the assumption that F is even in $\hat{\eta}$, it is straightforward to find a series solution to this equation with the asymptotic behaviour

$$F \sim -\ln|\hat{\eta}| \quad \text{as} \quad |\hat{\eta}| \to \infty\,. \tag{B 6}$$

The value of $F(0)$ is undetermined. Figure 8 shows the solution with $F(0) = 0$, together with $\hat{\eta}F'$.

A point in favour of this singularity is the relatively slow logarithmic growth in amplitude implied by (B 3), which seems consistent with our difficulty in confirming that numerical solutions to (B 2) become unbounded. However, it is possible that equation (B 2) admits other singularity structures with spanwise variations proportional to $(\bar{X}_s - \bar{X})^a$, $a < \frac{3}{4}$, and amplitude growth like $(\bar{X}_s - \bar{X})^{-3/4+a}$. If a singularity of the form (B 3)–(B 4) does indeed occur, then the relatively rapid contraction in the spanwise direction as $(\bar{X}_s - \bar{X})^{3/4}$ means that the asymptotically smaller $\hat{P}_{\hat{Z}\hat{Z}}$ term is growing in importance. Hence sufficiently close to the singularity it will be reinstated, and the governing equation will revert to (5.8) – without the $\bar{P}$ linear growth term (cf. §5.3).

We end this subsection by noting that equation (B 2) is no longer valid if the three-dimensionality is too weak. More precisely, when $\sigma^{25/4}\beta^{-1} \sim \sigma^5$, i.e. when

$\beta = O(\sigma^{5/4})$, the critical layer becomes strongly nonlinear as for a purely two-dimensional disturbance (e.g. Gajjar & Smith 1985; Goldstein & Durbin 1986).† The critical layer is surrounded by a diffusion layer (cf. Brown & Stewartson 1978; Churilov & Shukhman 1987; Goldstein & Hultgren 1988). However, in contrast to the purely two-dimensional case, the weak three-dimensional effects present for this distinguished scaling are likely to ensure that the diffusion layer is not passive.

B.2. *Strong spanwise variations*

If the spanwise variation is more rapid than that specified by (2.5), then it is necessary to specialize to particular types of spanwise dependence if linear disturbances are to be followed into the weakly nonlinear régime. To understand why this is so, note that the streamwise lengthscale is dictated by the growth rate provided by the Stokes layer. If the spanwise variation is more rapid than (2.5), then the $\partial^2 P_0/\partial Z^2$ term in (5.2) will be larger than the $\partial P_0/\partial X$ term, and the latter term cannot be retained in the leading-order amplitude equation; in general, this makes matching to an upstream linear stage impossible.‡ Nevertheless, we can consider stronger spanwise dependence in the particular cases where the disturbance in (5.2) consists essentially of an oblique mode, or a pair of oblique modes.

(*a*) A pure oblique mode satisfying (5.2) has the solution, $P_0 = \mathrm{e}^{\mathrm{i}\beta Z + (\kappa - \mathrm{i}d\beta^2)X/c_g}$; note that an additional frequency shift can be allowed, but can equally well be absorbed into the definition of ω (see the discussion leading up to (2.4)). Various modulations of this wave are possible, but a distinguished case has (i) the modulation travelling with the group velocity, and (ii) the 'spanwise' modulation perpendicular to the wavevector rather than the free stream. To this end we write

$$P_0 = \beta^{-1/2} P(\tau, X, \hat{Z}) \mathrm{e}^{\mathrm{i}\beta Z - \mathrm{i}d\beta^2 X/c_g} + \dots \,, \tag{B 7}$$

where $\tau = T - X/c_g$ is the retarded time variable, $\hat{Z} = (Z - 2d\beta T) - \alpha_0^{-1}\beta(X - c_g T)$ is the spanwise variable, and the scaled spanwise wavenumber is assumed to be large ($\beta \gg 1$). Then after use of (2.28), (5.4), etc., P is found to satisfy

$$c_g P_X - \mathrm{i}dP_{\hat{Z}\hat{Z}} = \kappa P + \mu P \frac{\partial}{\partial \hat{Z}} \int_0^\infty \zeta^{-1/2} |P|^2 (\tau - c_g^{-1}\zeta, X - \zeta, \hat{Z})\, \mathrm{d}\zeta \,. \tag{B 8}$$

A nonlinear term of similar form has been obtained in a related context by Churilov & Shukhman (1994), and also by Gajjar (private communication, 1994). Further discussion of equation (B 8) is given by Stewart & Wu (1996).

(*b*) For a pair of oblique modes, an appropriate substitution is

$$\begin{aligned} P_0 = {} & \beta^{-1} \mathrm{e}^{-\mathrm{i}d\beta^2 X/c_g} (P_{11}^+ \mathrm{e}^{\mathrm{i}\beta Z} + P_{11}^- \mathrm{e}^{-\mathrm{i}\beta Z}) \\ & + \beta^{-3} \mathrm{e}^{-\mathrm{i}d\beta^2 X/c_g} (P_{31}^+ \mathrm{e}^{\mathrm{i}\beta Z} + P_{31}^- \mathrm{e}^{-\mathrm{i}\beta Z} + P_{33}^+ \mathrm{e}^{3\mathrm{i}\beta Z} + P_{33}^- \mathrm{e}^{-3\mathrm{i}\beta Z}) + \dots \,, \end{aligned} \tag{B 9}$$

where $\beta \gg 1$, $\hat{z} = \beta^{-1} Z$, and the $P_{ij}^{\pm}$ are functions of T, X and $\hat{z}$. At leading order the

† A closely related three-dimensional scaling has been derived by Professor A. F. Messiter (private communication, 1991).

‡ However, if the requirement of linear upstream matching is relaxed, then it is possible to consider rapid spanwise modulations of more general form, e.g. Smith & Walton (1989).

amplitude equation (5.8) becomes

$$P_{11T}^{+} + c_g P_{11X}^{+} + 2dP_{11\hat{z}}^{+} = \kappa P_{11}^{+}$$
$$-2\mathrm{i}\mu P_{11}^{-} \int_0^{\infty} \zeta^{-1/2} P_{11}^{+}(T-\zeta/c_0, X-\zeta, \hat{z}) P_{11}^{-*}(T-\zeta/c_0, X-\zeta, \hat{z})\mathrm{d}\zeta \,, \qquad \text{(B 10)}$$

$$P_{11T}^{-} + c_g P_{11X}^{-} - 2dP_{11\hat{z}}^{-} = \kappa P_{11}^{-}$$
$$-2\mathrm{i}\mu P_{11}^{+} \int_0^{\infty} \zeta^{-1/2} P_{11}^{-}(T-\zeta/c_0, X-\zeta, \hat{z}) P_{11}^{+*}(T-\zeta/c_0, X-\zeta, \hat{z})\mathrm{d}\zeta \,. \qquad \text{(B 11)}$$

However, equations (B 10) and (B 11) are not valid for arbitrarily large β. Let us consider a fully three-dimensional problem where the T-S waves have an order-one obliqueness. The wall pressure might then take the form

$$P \sim \bar{\epsilon}\sigma(P_+(T,X,\bar{z})\mathrm{e}^{\mathrm{i}\bar{\xi}+\mathrm{i}\sigma\bar{\beta}z} + P_-(T,X,\bar{z})\mathrm{e}^{\mathrm{i}\bar{\xi}-\mathrm{i}\sigma\bar{\beta}z} + \text{c.c.}) + \dots \,, \qquad \text{(B 12)}$$

with

$$\bar{\xi} = \sigma\bar{\alpha}x - \sigma^2\omega t \,, \quad \bar{z} = \sigma^4 z \,, \quad \bar{\alpha} = \bar{\alpha}_0 + \sigma\bar{\alpha}_1 + \sigma^2\bar{\alpha}_2 + \sigma^3 \ln\sigma\bar{\alpha}_{3L} \,, \qquad \text{(B 13)}$$

and $\bar{\beta}$ of order one, in place of (2.9). Equation (B 12) represents two oblique modes with comparable streamwise and spanwise wavenumbers, propagating at equal and opposite angles to the flow direction. In this case, by a slight modification of the work of Mankbadi *et al.* (1993) and Wu (1993*b*), we find that when $\bar{\epsilon} = O(\sigma^8)$ the leading–order dispersion relation is

$$\bar{\alpha}_0\left(\bar{\alpha}_0^2 + \bar{\beta}^2\right)^{1/2} = \lambda\omega \,, \qquad \text{(B 14)}$$

and the governing amplitude-evolution equations are

$$\frac{\partial P_+}{\partial T} + \bar{c}_{gx}\frac{\partial P_+}{\partial X} + \bar{c}_{gz}\frac{\partial P_+}{\partial \bar{z}} = \bar{\kappa}P_+$$
$$-\mathrm{i}\bar{\beta}^4\bar{\mu}P_- \int_0^{\infty} P_+(T-\zeta/\bar{c}_0, X-\zeta, \bar{z}) P_-^*(T-\zeta/\bar{c}_0, X-\zeta, \bar{z})\mathrm{d}\zeta \,, \qquad \text{(B 15)}$$

$$\frac{\partial P_-}{\partial T} + \bar{c}_{gx}\frac{\partial P_-}{\partial X} - \bar{c}_{gz}\frac{\partial P_-}{\partial \bar{z}} = \bar{\kappa}P_-$$
$$-\mathrm{i}\bar{\beta}^4\bar{\mu}P_+ \int_0^{\infty} P_+^*(T-\zeta/\bar{c}_0, X-\zeta, \bar{z}) P_-(T-\zeta/\bar{c}_0, X-\zeta, \bar{z})\mathrm{d}\zeta \,, \qquad \text{(B 16)}$$

where $\bar{z} = \sigma^4 z$ represents a slow spanwise modulation, and

$$\bar{c}_0 = \omega/\bar{\alpha}_0 \,, \quad \bar{c}_{gx} = \bar{\alpha}_0(\cos\bar{\theta} + \sec\bar{\theta})/\lambda \,, \quad \bar{c}_{gz} = \bar{\alpha}_0 \sin\bar{\theta}/\lambda \,, \qquad \text{(B 17)}$$

$$\bar{\mu} = \frac{8\pi\bar{c}_0}{2^{1/3}(3\bar{\alpha}_0)^{2/3}\lambda^{8/3}}\Gamma(\tfrac{1}{3})\cos 2\bar{\theta} \,, \quad \bar{\theta} = \tan^{-1}(\bar{\beta}/\bar{\alpha}_0) \,. \qquad \text{(B 18)}$$

The systems of equations (B 10), (B 11) and (B 15), (B 16) clearly differ. This indicates that there is an intermediate scaling between the $\bar{\beta} = O(\sigma^{3/2})$ scale considered in this paper, and the $\bar{\beta} = O(1)$ scale considered by Mankbadi *et al.* (1993) and Wu (1993*b*). We identify this intermediate scaling to be $\bar{\beta} = O(\sigma^{1/4})$. For such moderately oblique waves, we introduce

$$\tilde{\beta} = \sigma^{-1/4}\bar{\beta} \,, \quad \tilde{z} = \sigma^{15/4}\tilde{\beta}^{-1}z \,, \quad P_{\pm}(T,X,\tilde{z}) = \sigma^{1/2}\tilde{\beta}P_{\pm}(T,X,z). \qquad \text{(B 19)}$$

Then by combining the analysis in the present paper with that of Wu *et al.* (1993),

Mankbadi *et al.* (1993) and Wu (1993*b*), we have that

$$\frac{\partial \tilde{P}_+}{\partial T} + c_g \frac{\partial \tilde{P}_+}{\partial X} + 2d\frac{\partial \tilde{P}_+}{\partial \tilde{z}} = \kappa \tilde{P}_+ - \mathrm{i}\tilde{P}_- \int_0^\infty K(\zeta)\tilde{P}_+(T-\zeta/c_0, X-\zeta, \tilde{z})\tilde{P}_-^*(T-\zeta/c_0, X-\zeta, \tilde{z})\mathrm{d}\zeta \,, \tag{B 20}$$

$$\frac{\partial \tilde{P}^-}{\partial T} + c_g \frac{\partial \tilde{P}_-}{\partial X} - 2d\frac{\partial \tilde{P}_-}{\partial \tilde{z}} = \kappa \tilde{P}_- - \mathrm{i}\tilde{P}_+ \int_0^\infty K(\zeta)\tilde{P}_+^*(T-\zeta/c_0, X-\zeta, \tilde{z})\tilde{P}_-(T-\zeta/c_0, X-\zeta, \tilde{z})\mathrm{d}\zeta \,, \tag{B 21}$$

where

$$K(\zeta) = 2\mu\zeta^{-1/2} + \tilde{\beta}^2\bar{\mu}_0 \,, \qquad \bar{\mu}_0 = \frac{8\pi c_0}{2^{1/3}(3\alpha_0)^{2/3}\lambda^{8/3}}\Gamma(\tfrac{1}{3}) \,. \tag{B 22}$$

Clearly, this system of equations reduces to (B 10), (B 11) in the limit $\tilde{\beta} \to 0$, while as $\tilde{\beta} \to \infty$ it matches to the small-$\bar{\beta}$ limit of (B 15), (B 16).

For all $\tilde{\beta}$, the coefficients of the nonlinear terms in (B 20) and (B 21) are purely imaginary. It follows that if $\tilde{P}_\pm$ are periodic in $\tilde{z}$, with period $\tilde{L}$, the 'energy' integral

$$E(T,X) = \int_0^{\tilde{L}} \left(|\tilde{P}_+|^2 + |\tilde{P}_-|^2\right) \mathrm{d}\tilde{z} \tag{B 23}$$

satisfies

$$\left(\frac{\partial}{\partial T} + c_g\frac{\partial}{\partial X}\right) E = 2\kappa_R E \,. \tag{B 24}$$

If instead equations (B 20)–(B 22) describe a pair of localized wavepackets, so that $\tilde{P}_\pm \to 0$ as $|\tilde{z}| \to \infty$, then (B 23)–(B 24) holds with $\int_0^{\tilde{L}}$ replaced by $\int_{-\infty}^{\infty}$. In both cases the 'energy' grows exponentially in a frame moving downstream with the group velocity.

For the particular case where the $\tilde{P}_\pm$ are independent of $\tilde{z}$, equations (B 20)–(B 22) admit an exact, equal-amplitude solution

$$\tilde{P}_+ = \tilde{P}_- = R(\tau)\exp(\kappa X/c_g + \mathrm{i}\Theta) \,, \quad \tau = T - X/c_g \,, \tag{B 25}$$

$$\Theta(T,X) = \Theta_0(\tau) - (2\kappa_R)^{-1}\int_0^\infty K(\zeta)\exp\left[2\kappa_R(X-\zeta)/c_g\right]R^2\left(\tau - \zeta/c_g\right)\mathrm{d}\zeta \,, \tag{B 26}$$

where R and Θ_0 are arbitrary real-valued functions. Numerical solutions of (B 20)–(B 22) with the $\tilde{P}_\pm$ functions of X only (or of T only), and with unequal initial amplitudes, have been found by Wu (1993*b*) in the large-$\tilde{\beta}$ limit. He finds that the equal-amplitude state (B 25)–(B 26) is attained at large X (or T). Further computations under the same assumptions suggest that this is so for all values of $\tilde{\beta}$. Work is in progress to investigate solutions of the full system (B 20)–(B 22) (Jennings *et al.* 1996). The same equations, with more general complex values for μ and $\bar{\mu}_0$ (cf. Wu 1993*a*, *b*), and allowing for weak non-parallelism, have been studied by Timoshin & Smith (1993).

Finally, we note that asymptotic description (B 9)–(B 11) will not be valid for arbitrarily large X, since it is readily shown that if the $P_{11}^\pm$ grow like $\mathrm{e}^{\gamma X}$, the third-harmonic terms $P_{33}^\pm$ behave like $\mathrm{e}^{3\gamma X}$. In fact, all (odd) harmonics become significant at leading order when $X = O(\ln\beta)$, and the subsequent development is described by equation (5.2), without the linear growth term.

Appendix C. Numerical method for (5.32)

Rather than solving (5.32) in complex form, we first write

$$G = \rho \exp(\mathrm{i}\phi)\,, \tag{C 1}$$

where ρ and ϕ are real variables which satisfy

$$\tfrac{1}{4}\rho + \tfrac{1}{2}\eta\rho' + 2\rho'\phi' + \rho\phi'' = \rho \int_0^\eta \frac{2\xi(\rho^2(\xi)\phi'(\xi))'}{\eta(\eta^2 - \xi^2)^{1/2}}\,\mathrm{d}\xi\,, \tag{C 2}$$

$$-K\rho + \tfrac{1}{2}\eta\rho\phi' - \rho'' + \rho(\phi')^2 = \rho \int_0^\eta \frac{2\xi(\rho(\xi)\rho'(\xi))'}{\eta(\eta^2 - \xi^2)^{1/2}}\,\mathrm{d}\xi\,. \tag{C 3}$$

We seek solutions that are even in η and for which

$$\rho \to 0\,, \quad \phi' \to 0 \quad \text{as} \quad |\eta| \to \infty\,. \tag{C 4}$$

Equations (C 2) and (C 3) were solved using a modified fourth-order Runge–Kutta scheme. The solution was marched in the direction of increasing η starting from the series solution at $\eta = \eta_0 > 0$. The integrals were evaluated using Simpson's rule after making the transformation $\xi = \eta \sin\psi$. The end point at $\xi = \eta$, i.e. $\psi = \pi/2$, was incorporated explicitly into the Runge–Kutta scheme, although extrapolation from the solution at previous grid points was necessary to calculate the integrands at certain points. The extrapolation tended to leave the numerical scheme unstable, and hence a 'corrector' step was implemented in which only interpolation was necessary in the calculation of the integrands. At the Nth step of the Runge–Kutta scheme, approximately $3N$ (even) intervals were used in Simpson's rule. The numerical scheme was tested against the exact solution

$$\rho = \tfrac{1}{2}\,, \quad \phi' = -\tfrac{1}{2}\eta\,, \quad K = 0\,. \tag{C 5}$$

The solution in figure 6 for $K = 0.392751$ and $G(0) = 0.986440$ was plotted using 60 terms of the series solution at $\eta_0 = 0.4$, and a step size of $h = 0.01$.

REFERENCES

Bassom, A. P. & Hall, P. 1991 Concerning the interaction of non-stationary cross-flow vortices in a three-dimensional boundary layer. *Q. J. Mech. Appl. Maths* **44**, 147–172.

Bender, C. M. & Orszag, S. 1978 *Advanced Mathematical Methods for Scientists and Engineers.* McGraw-Hill.

Bodonyi, R. J. & Smith, F. T. 1981 The upper-branch stability of the Blasius boundary layer, including non-parallel flow effects. *Proc. R. Soc. Lond.* A **375**, 65–92.

Brown, P. G., Brown, S. N., Smith, F. T. & Timoshin, S. N. 1993 On the starting process of strongly nonlinear vortex/Rayleigh-wave interactions. *Mathematika* **40**, 7–29.

Brown, S. N. & Stewartson, K. 1978 The evolution of the critical layer of Rossby wave, Part II. *Geophys. Astrophys. Fluid Dyn.* **10**, 1–24.

Churilov, S. M. & Shukhman, I. G. 1987 Nonlinear stability of a stratified shear flow: a viscous critical layer. *J. Fluid Mech.* **180**, 1–20.

Churilov, S. M. & Shukhman, I. G. 1988 Nonlinear stability of a stratified shear flow in the regime with an unsteady critical layer. *J. Fluid Mech.* **194**, 187–216.

Churilov, S. M. & Shukhman, I. G. 1994 Nonlinear spatial evolution of helical disturbance disturbances to an axial jet. *J. Fluid Mech.* **281**, 371–402.

Cohen, J., Breuer, K. S. & Haritonidis, J. H. 1991 On the evolution of a wavepacket in a laminar boundary layer. *J. Fluid Mech.* **225**, 575–606.

Cowley, S. J. 1981 High Reynolds number flows through distorted channels and flexible tubes. PhD thesis, University of Cambridge.

COWLEY, S. J. & WU, X. 1994 Asymptotic approaches to transition modelling. In *Progress in Transition Modelling, AGARD Rep.* 793, Chap. 3, pp. 1–38.

CRAIK, A. D. D. 1971 Non-linear resonant instability in boundary layers. *J. Fluid Mech.* **50**, 393–413.

DAVEY, A., HOCKING, L. M. & STEWARTSON, K. 1974 On the nonlinear evolution of three-dimensional disturbances in plane Poiseuille flow. *J. Fluid. Mech.* **63**, 529–536.

GAJJAR, J. S. B. & SMITH, F. T. 1985 On the global instability of free disturbances with a time-dependent nonlinear viscous critical layer. *J. Fluid Mech.* **157**, 53–77.

GASTER, M. 1975 An theoretical model for the development of a wave packet in a laminar boundary layer. *Proc. R. Soc. Lond.* A **347**, 271–289.

GASTER, M. & GRANT, I. 1975 An experimental investigation of the formation and development of a wave packet in a laminar boundary layer. *Proc. R. Soc. Lond.* A **347**, 253–269.

GOLDSTEIN, M. E. & CHOI, S.-W. 1989 Nonlinear evolution of interacting oblique waves on two-dimensional shear layers. *J. Fluid Mech.* **207**, 97–120 and Corrigendum *J. Fluid Mech.* **216**, 1990, 659–663.

GOLDSTEIN, M. E. & DURBIN, P. A. 1986 Nonlinear critical layers eliminate the upper branch of spatially growing Tollmien-Schlichting waves. *Phys. Fluids* **29**, 2344–2345.

GOLDSTEIN, M. E. & HULTGREN, L. S. 1988 Nonlinear spatial evolution of an externally excited instability wave in a free shear layer. *J. Fluid Mech.* **245**, 523–551.

GOLDSTEIN, M. E. & HULTGREN, L. S. 1989 Boundary-layer receptivity to long-wave free-stream disturbances. *Ann. Rev. Fluid Mech.* **21**, 137–166.

GOLDSTEIN, M. E. & LEE, S. S. 1992 Fully coupled resonant-triad interaction in an adverse-pressure-gradient boundary layer. *J. Fluid Mech.* **245**, 523–551.

GOLDSTEIN, M. E. & LEIB, S. J. 1989 Nonlinear evolution of oblique waves on compressible shear layers. *J. Fluid Mech.* **207**, 73–96.

HABERMAN, R. 1972 Critical layers in parallel flows. *Stud. Appl. Maths* **50**, 139–161.

HALL, P. 1995 A phase-equation approach to boundary-layer instability theory: Tollmien-Schlichting waves. *J Fluid Mech.* **304**, 185–212.

HALL, P. & SMITH, F. T. 1989 Nonlinear Tollmien-Schlichting/vortex interaction in boundary layers. *Eur. J. Mech.* B **8**, 179–205.

HALL, P. & SMITH, F. T. 1990 Near-planar TS waves and longitudinal vortices in channel flows: nonlinear interaction and focussing. In *Instability and Transition II* (ed. M.Y. Hussaini & R.G. Voigt). Springer.

HALL, P. & SMITH, F. T. 1991 On strongly nonlinear vortex/wave interactions in boundary-layer transition. *J. Fluid Mech.* **227**, 641–666. See also *ICASE Rep.* 89-22.

HAYNES, P. H. & COWLEY, S. J. 1986 The evolution of an unsteady translating nonlinear Rossby-wave critical layer. *Geophys. Astrophys. Fluid Dyn.* **35**, 1–55.

HEALEY, J. J. 1995 On the neutral curve of the flat-plate boundary layer: comparison between experiment, Orr–Sommerfeld theory and asymptotic theory. *J. Fluid Mech.* **288**, 59–83.

HERBERT, T. 1983 Secondary instability of plane channel flow to subharmonic three-dimensional disturbances. *Phys. Fluids* **26**, 871–874.

HERBERT, T. 1988 Secondary instability of boundary layers. *Ann. Rev. Fluid Mech.* **20**, 487–526.

HICKERNELL, F. J. 1984 Time-dependent critical layers in shear flows on the beta-plane. *J. Fluid Mech.* **142**, 431–449.

HOCKING, L. M. 1975 Non-linear instability of the asymptotic suction velocity profile. *Q. J. Mech. Appl. Maths* **28**, 341–353

HOCKING, L. M., STEWARTSON, K. & STUART, J. T. 1972 A nonlinear instability burst in plane parallel flow. *J. Fluid Mech.* **51**, 705–735.

KACHANOV, YU. S. & LEVCHENKO, V. YA. 1984 The resonant interaction of disturbances at laminar-turbulent transition in a boundary layer. *J. Fluid Mech.* **138**, 209–247.

KHOKHLOV, A. P. 1991 The temporal evolution of Tollmien-Schlichting waves near nonlinear resonance. Preprint.

KHOKHLOV, A. P. 1993 Evolution of resonant triads in a boundary layer. Submitted to *J. Fluid Mech.*

KLEBANOFF, P. S. & TIDSTROM, K. D. 1959 The evolution of amplified waves leading to transition in a boundary layer with zero pressure gradient. *Tech. Notes Natl Aero. Space Admin., WA.* D-195.

KLEBANOFF, P. S., TIDSTROM, K. D. & SARGENT, L. M. 1962 The three-dimensional nature of boundary layer instability. *J. Fluid Mech.* **12**, 1–34.

KRASNY, R. 1986 A study of singularity formation in a vortex sheet by the point-vortex approximation. *J. Fluid Mech.* **167**, 65–93.

LEIB, S. J. 1991 Nonlinear evolution of subsonic and supersonic disturbances on a compressible free shear layer. *J. Fluid Mech.* **224**, 551–578.

MANKBADI, R. R. 1991 Resonant triad in boundary-layer instability. *NASA TM*-105208.

MANKBADI, R. R., WU, X. & LEE, S. S. 1993 A critical-layer analysis of the resonant triad in Blasius boundary-layer transition: nonlinear interactions. *J. Fluid Mech.* **256**, 85–106.

NISHIOKA, M., ASAI, N. & IIDA, S. 1979 In *Laminar-Turbulence Transition, IUTAM Symp.*, Stuttgart (ed. R. Eppler & H. Fasel). Springer.

RAETZ, G. S. 1959 A new theory of the cause of transition in fluid flows. *Norair Rep.* NOR-59-383, Hawthorne, CA.

REID, W. H. 1965 The stability of parallel flows. In *Basic Developments in Fluid Dynamics* (ed. M. Holt), pp. 249–308. Academic,

SARIC, W. S. & THOMAS, A. S. W. 1984 Experiments on subharmonic route to turbulence in boundary layers. In *Turbulence and Chaotic Phenomena in Fluids* (ed. T. Tatsumi) pp. 117–22. North-Holland.

SHUKHMAN, I. G. 1991 Nonlinear evolution of spiral density waves generated by the instability of the shear-layer in a rotating compressible fluid. *J. Fluid Mech.* **233**, 587–612.

SMITH, F. T. 1979 On the non-parallel flow instability of the Blasius boundary layer. *Proc. R. Soc. Lond.* A **336**, 91–109.

SMITH, F. T. 1986 The strong nonlinear growth of three-dimensional disturbances in boundary layers. *Utd. Tech. Res. Cent., E. Hartford, CT, Rep.* UTRC-86-10.

SMITH, F. T. 1992 On nonlinear effects near the wing-tips of an evolving boundary-layer spot. *Phil. Trans. R. Soc. Lond.* A **340**, 131–165.

SMITH, F. T. & BLENNERHASSETT, P. 1992 Nonlinear interaction of oblique three-dimensional Tollmien-Schlichting waves and longitudinal vortices, in channel flows and boundary layers. *Proc. R. Soc. Lond.* A **436**, 585–602.

SMITH, F. T. & BODONYI, R. J. 1982 Nonlinear critical layers and their development in streaming-flow stability. *J. Fluid Mech.* **118**, 165–185.

SMITH, F. T. & BOWLES, R. I. 1992 Transition theory and experimental comparisons on (I) amplification into streets and (II) a strongly nonlinear break-up criterion. *Proc. R. Soc. Lond.* A **439**, 163–175.

SMITH, F. T., BROWN, S. N. & BROWN, P. G. 1993 Initiation of three-dimensional nonlinear transition paths from an inflectional profile. *Eur. J. Mech.* B **12**, 447–473.

SMITH, F. T. & BURGGRAF, O. R. 1985 On the development of large-sized short-scaled disturbances in boundary layers. *Proc. R. Soc. Lond.* A **399**, 25–55.

SMITH, F. T. & STEWART, P. A. 1987 The resonant-triad nonlinear interaction in boundary-layer transition. *J. Fluid Mech.* **179**, 227–252.

SMITH, F. T., STEWART, P. A. & BOWLES, R. G. A. 1994 On the nonlinear growth of single three-dimensional disturbances in boundary layers. *Mathematika* **41**, 1–39.

SMITH, F. T. & WALTON, A. G. 1989 Nonlinear interaction of near-planar TS waves and longitudinal vortices in boundary-layer transition. *Mathematika* **36**, 262–289.

STEWART, P. A. & SMITH, F. T. 1987 Three-dimensional instabilities in steady and unsteady non-parallel boundary layers, including effects of Tollmien-Schlichting disturbances and cross flow. *Proc. R. Soc. Lond.* A **409**, 229–248.

STEWART, P. A. & SMITH, F. T. 1992 Three-dimensional nonlinear blow-up from a nearly planar initial disturbance, in boundary-layer transition: theory and experimental comparisons. *J. Fluid Mech.* **244**, 79–100.

STEWARTSON, K. 1978 The evolution of the critical layer of a Rossby wave. *Geophys. Astrophys. Fluid Dyn.* **9**, 185–200.

STEWARTSON, K. & STUART, J. T. 1971 A nonlinear instability theory for a wave system in plane Poiseuille flow. *J. Fluid Mech.* **48**, 529–545.

STUART, J. T. & DIPRIMA, R. C. 1978 The Eckhaus and Benjamin-Feir resonance mechanism. *Proc. R. Soc. Lond.* A **362**, 27–41.

TIMOSHIN, S. N. & SMITH, F. T. 1993. On the nonlinear vortex-Rayleigh wave interaction in

a boundary-layer flow. Presented at the *International Workshop on Advances in Analytical Methods in Aerodynamics, 12-14 July 1993, Miedzyzdroje, Poland.*

WU, X. 1992 The nonlinear evolution of high-frequency resonant-triad waves in an oscillatory Stokes-layer at high Reynolds number. *J. Fluid Mech.* **245**, 553–597.

WU, X. 1993*a* Nonlinear temporal-spatial modulation of near-planar Rayleigh waves in shear flows: formation of streamwise vortices. *J. Fluid Mech.* **256**, 685–719.

WU, X, 1993*b* On critical-layer and diffusion-layer nonlinearity in the three-dimensional stage of boundary-layer transition. *Proc. R. Soc. Lond.* A **443**, 95–106.

WU, X., LEE, S. S. & COWLEY, S. J. 1993 On the weakly nonlinear three-dimensional instability of shear flows to pairs of oblique waves: the Stokes layer as a paradigm. *J. Fluid Mech.*, **253**, 681–721. See also *NASA TM*-105918, *ICOMP*-92-20.

WU, X. & STEWART, P. A. 1996 Interaction of phase-locked modes: a new mechanism for the rapid growth of three-dimensional disturbances. *J. Fluid Mech.* **316**, 335–372.

WUNDROW, D. W., HULTGREN, L. S. & GOLDSTEIN, M. E. 1994 Interaction of oblique instability waves with a nonlinear plane wave. *J. Fluid Mech.* **264**, 343–372.

ZELMAN, M. B. & MASLENNIKOVA, I. I. 1993 Tollmien-Schlichting-wave resonant mechanism for subharmonic-type transition. *J. Fluid Mech.* **252**, 449–478.

ZHUK, V. I. & RYZHOV, O. S. 1982 On locally-inviscid disturbances in boundary layer with self-induced pressure. *Dokl. Akad. Nauk. SSSR* **263**(1), 56–69.